Received: 21 July 2020 | Revised: 12 September 2020 | Accepted: 20 September 2020

DOI: 10.1002/jmor.21276

RESEARCH ARTICLE

JOURNAL OF morphology WILEY

Ultrastructure of chemosensory tarsal tip-pore sensilla of *Argiope* spp. Audouin, 1826 (Chelicerata: Araneae: Araneidae)

Carsten H. G. Müller | Anne-Sarah Ganske | Gabriele Uhl

Department of General and Systematic Zoology, Zoological Institute and Museum, University of Greifswald, Greifswald, Germany

Correspondence
Carsten H. G. Müller, Department of General and Systematic Zoology, Zoological Institute and Museum, University of Greifswald, Loitzer Str. 26, 17489 Greifswald, Germany.
Email: carstmue@uni-greifswald.de

Abstract

While chemical communication has been investigated intensively in vertebrates and insects, relatively little is known about the sensory world of spiders despite the fact that chemical cues play a key role in natural and sexual selection in this group. In insects, olfaction is performed with wall–pore and gustation with tip-pore sensilla. Since spiders possess tip-pore sensilla only, it is unclear how they accomplish olfaction. We scrutinized the ultrastructure of the trichoid tip-pore sensilla of the orb weaving spider *Argiope bruennichi*—a common Palearctic species the males of which are known to be attracted by female sex pheromone. We also investigated the congener *Argiope blanda*. We examined whether the tip-pore sensilla differ in ultrastructure depending on sex and their position on the tarsi of walking legs of which only the distal parts are in contact with the substrate. We hypothesized as yet undetected differences in ultrastructure that suggest gustatory versus olfactory functions. All tarsal tip-pore sensilla of both species exhibit characters typical of contact-chemoreceptors, such as (a) the presence of a pore at the tip of the sensillum shaft, (b) 2–22 uniciliated chemoreceptive cells with elongated and unbranched dendrites reaching up to the tip-pore, (c) two integrated mechanoreceptive cells with short dendrites and large tubular bodies attached to the sensillum shaft's base, and (d) a socket structure with suspension fibres that render the sensillum shaft flexible. The newly found third mechanoreceptive cell attached to the proximal end of the peridendritic shaft cylinder by a small tubular body was likely overlooked in previous studies. The organization of tarsal tip-pore sensilla did not differ depending on the position on the tarsus nor between the sexes. As no wall-pore sensilla were detected, we discuss the probability that a single type of sensillum performs both gustation and olfaction in spiders.

KEYWORDS

electron microscopy, gustation, mechanoreception, olfaction, spiders

1 | INTRODUCTION

Animals rely on a wide range of sensory systems for foraging, predator avoidance, finding shelter, suitable habitats and for attracting and choosing mating partners. Although the visual and auditory senses are much better explored, the chemical sense plays a pivotal role in all living beings from bacteria to vertebrates (Wyatt, 2003). Since chemical cues and signals are not visible and tangible, making their exploration

more difficult, research has been focusing on vertebrates for reasons of similarity to humans and on insects for reasons of pest control (Symonds & Elgar, 2008).

In arthropods, sensing of most modalities is achieved with the aid of cuticular sensilla. Primary receptor cells below the cuticle form modified ciliary processes, which are composed of the basal ciliary segment and the distal dendritic outer segment. The dendritic outer segment carries receptors that transduce environmental stimuli into bioelectric signals (e.g., Altner & Prillinger, 1980; Steinbrecht, 1984). Cuticular sensilla may perform mechanoreception, hygroreception, reception of CO_2, thermoreception, reception of electric fields, contact-chemoreception (gustation), or chemoreception over a distance (olfaction). Receptor modalities can be elucidated by conducting electrophysiological recordings, molecular genetic analyses or by finding modality-specific ultrastructures using transmission electron microscopy (TEM; Altner & Prillinger, 1980; Zacharuk, 1980; Keil & Steinbrecht, 1984; Altner & Loftus, 1985; Tichy & Barth, 1992; Tichy & Loftus, 1996; Ozaki & Tominaga, 1999; Steinbrecht, 1997, 1999; Iwasaki, Itoh, & Tominaga, 1999; Yokohari, 1999; Keil, 2012). A revealing ultrastructure, for example, for mechanoreception is the tubular body at the tip of a short dendritic outer segment. This tubular body connects to a movable socket of a trichoid sensillum (e.g., Keil & Steinbrecht, 1984). Chemosensory sensilla are characterized by pores in the cuticle of the sensillum shaft that allow chemicals to reach the receptors. Receptors are incorporated in the membrane of the elongated dendritic outer segment that projects into the sensillum shaft. In insects, gustation and olfaction are performed with two different types of sensilla. For contact-chemoreception, socketed and single-pored trichoid sensilla (tip-pore sensilla) are used, which include multiple dendritic outer segments that reach up to the terminal pore where they receive soluble chemicals. In contrast, air-borne chemicals are transferred through multiple pores along the entire, unsocketed shaft of wall-pore or multiporous sensilla (single- or double-walled) (Hunger & Steinbrecht, 1998; Meinecke, 1975; Steinbrecht, 1999). Odorants pass through pore tubules or spoke channels and connect to the often branched dendritic outer segments (see Steinbrecht, 1999 for review). Tip-pore sensilla are known to be present in most arachnid taxa (e.g., Talarico, Palacios-Vargas, Fuentes Silva, & Alberti, 2006; Talarico, Palacios-Vargas, & Alberti, 2008; and review by Foelix, 1985), whereas single- or double-walled multiporous sensilla with branched or unbranched dendrites have only been reported from Opiliones, Amblypygi, Ricinulei, and Acari (e.g., Foelix & Axtell, 1972; Foelix, Chu-Wang, & Beck, 1975; Gainett et al., 2017; Hess & Vlimant, 1982; Talarico et al., 2006, 2008). In spiders and scorpions, however, multiporous sensilla seem to be extremely rare or even absent (Farley, 1999; Foelix, 1985).

Previous studies showed that spiders possess tip-pore sensilla only (e.g., Foelix, 1970, 2011, 2015; Foelix & Chu-Wang, 1973a; Foelix, Erb, & Rast, 2013; Ganske & Uhl, 2018; Harris & Mill, 1973; Kronestedt, 1979; Pfreundt & Peters, 1981; Ross & Smith, 1979; Tichy, Gingl, Ehn, Papke, & Schulz, 2001), with one possible exception in a species-poor and basally branching off taxon (Foelix et al., 1975). Consequently, based on the anatomical equipment alone, one might assume that spiders are not able to perceive volatile odours. The so-called tarsal organ, which occurs singly on the tarsus of each leg and pedipalp (e.g., Anton & Tichy, 1994; Foelix, 1985; Forster, 1980; Forster, Platnick, & Gray, 1987; Tichy & Barth, 1992), was previously considered an olfactory organ (Dumpert, 1978; "pheromone receptor": Foelix, 1992) but was found to act as a hygroreceptor (Ehn & Tichy, 1994; Tichy & Barth, 1992; Tichy & Loftus, 1996). In marked contrast to the morphological findings, a wealth of behavioural observations clearly demonstrate that spiders are able to smell (e.g., Blanke, 1973; Gaskett, 2007; Uhl, 2013; Uhl & Elias, 2011; Witt, 1982). Spiders use volatile odours to detect prey and mates over large distances (Gaskett, 2007; Uhl, 2013; Uhl & Elias, 2011) and for a few spider species, the pheromones were identified and tested in bioassays (review in Uhl, 2013; Fischer, Lee, Stewart, & Gries, 2019). Nevertheless, how spiders smell has remained a conundrum.

Spiders of the genus *Argiope* Audouin, 1826 (Araneidae) are ideal models to unravel the chemical sense of spiders, since their mating behaviour has been studied intensively in the laboratory and under natural conditions (Schneider, Uhl, & Herberstein, 2015). *Argiope bruennichi* lends itself as a focal species because the sex pheromone has been identified, synthesized and successfully tested in the field. The trimethyl methylcitrate attracts males over large distances and elicits courtship behaviour (Chinta et al., 2010). Furthermore, an atlas of the distribution of all sensillum types of *A. bruennichi* based on scanning electron microscopy (SEM) is now available (Ganske & Uhl, 2018). The study confirms that both sexes possess only tip-pore sensilla as chemoreceptors, as no wall-pore sensillum could be found with SEM (Ganske & Uhl, 2018). Since the trichoid tip-pore sensilla are not only abundant in regions that contact the substrate but occur on all podomeres of the legs, Ganske and Uhl (2018) proposed that these sensilla may either receive and transduce both olfactory and gustatory stimuli or show cryptic ultrastructural differences depending on their position on the leg.

In this study, we examine the organization of the trichoid tip-pore sensilla of *A. bruennichi* using SEM, semi-thin histology and TEM. We describe the ultrastructure of these sensilla along the tarsi of the first and second walking legs and assess whether there are areas of the sensillum shaft potentially permeable to volatile odours, but not visible using the SEM. We paid particular attention to potential differences in ultrastructural composition depending on the sensillum's location and orientation on the tarsus (towards and away from the substrate). By using males and females, we further analysed if the sexes differ in the ultrastructure of their tip-pore sensilla. We further inspected the New World congener *Argiope blanda* in order to assess whether there are species-specific differences in sensillum organization.

2 | MATERIALS AND METHODS

2.1 | Field collection and dissection

Adult females and males of *A. bruennichi* (Scopoli, 1772) were collected in July and August 2017 on meadows near Greifswald

(Germany). Adult females of *A. blanda* O. Pickard-Cambridge, 1898 were collected nearby Playa Panama (Guanacaste, Costa Rica, pasaporte Cientifico 01334 of GU). Prior to dissection and preparation for histology and electron microscopy, all investigated specimens were anaesthetized with CO_2.

2.2 | Scanning electron microscopy

Adult specimens of *A. bruennichi* (five females, two males) were used for SEM. The first and second walking legs of *A. bruennichi* were chemically fixed with 80% ethanol for at least 24 hr. After cleaning the fixed legs in an ultrasonic bath, they were dehydrated in a graded series of ethanol, and critical-point-dried using a BAL-TEC CPD 030 or a LEICA EM CPD300. Critical-point-dried legs were mounted on carriers according to Ganske and Uhl (2018), sputter-coated with gold–palladium (ratio: 80/20; Polaron SC7640, Fisons Instruments) and examined with a ZEISS EVO LS10 at an accelerating voltage of 10 kV at the Imaging Center of the University of Greifswald. The distribution of tip-pore sensilla on tarsi of first and second walking legs was investigated in *A. bruennichi* using SEM. The distribution of tip-pore sensilla of *A. blanda* was assessed and compared with *A. bruennichi* using a SZH-10 stereomicroscope (Olympus). Detailed description and morphometric measurements of the shaft surface of the tip-pore sensilla were undertaken for *A. bruennichi* on the tarsi of second walking legs of a single specimen (~20 sensilla examined).

2.3 | TEM and histology

First and second walking legs of four females and three males of *A. bruennichi* as well as of three females of *A. blanda* were taken from the anaesthetized animal with micro-scissors, while it was placed in ice-cold prefixative modified after Karnovsky (1965) containing 2.5% glutaraldehyde, 2.5% paraformaldehyde, 1.5% NaOH, and 1,5% D-glucose (in 0.1 mol/L sodium phosphate buffer, pH 7.4). Tarsi were cut into two (distal and proximal) pieces of about 1–2 mm in length in the same prefixative to facilitate chemical fixation. Incubation was maintained for approximately 30 min. To enhance fixation quality and tissue contrast, we then applied 3 × 2 min pulses of microwave radiation (operated at a power of 200 W or 300 W) generated by a PELCO BioWave Pro (equipped with the solid state cooling unit PELCO SteadyTemp Pro Thermo Cube). Sample temperature was monitored and ranged between 8–10°C prior and 23–27°C after BioWave application. Tarsal pieces were then kept overnight in the same prefixative in a lightproof box at room temperature. After rinsing three times for 5 min in buffer solution in 0.1 mol/L sodium phosphate buffer (pH 7.4), postfixation in 2% OsO_4 solution was conducted at room temperature for 3 hr, followed by dehydration in graded series of ethanols and then transferred to propylene oxide. In order to replace propylene oxide with the embedding medium EmBed 812 resin and to remove tissue-enclosed gases, pre-embedding steps (ratio propylenoxide versus resin: 2:1 for 4 hr; 1:1 for 12 hr; 1:2 for 12 hr, 100% resin for 1 hr) were carried out. Pre-embedding in 100% resin was prolonged for further 60 min in a HERAEUS VT-6025 vacuum drying cabinet (operated at 150 mbar and 40°C). Vacuum exposition was arranged in three steps of 20 min steps with 5 min breaks in between under normal atmospheric pressure. After each step, the vacuum was released slowly and bubbles of residual, gaseous propylene oxide leaking from the tarsal pieces were removed. Then, the tarsal pieces were transferred to the embedding molts that contained new resin. Tarsi were oriented in the resin block with their lateral or dorsal side facing the cutting edge. Polymerization of the resin blocks was carried out in a heating cabinet at 60°C for a minimum of 24 hr.

On each tarsal piece, 20–30 tip-pore sensilla could be analysed. Only those tip-pore sensilla with their shafts oriented perpendicular to the cutting edge provided suitable cross sections that enabled us to assess the number of chemoreceptive dendritic outer segments in a given sensillum. Tip-pore sensilla on the ventral and lateral side of the tarsus were considered as sensilla that touch the substrate and are used for gustation, whereas those located on the dorsal side face away from the substrate and were thus considered as candidates of olfactory sensilla.

Transverse and horizontal ultra-thin sections (55–70 nm) of the tarsal pieces were made using a LEICA UCT ultramicrotome. Series of ultra-thin sections alternated with two semi-thin sections (700 nm in thickness), which were taken every 5 μm for orientation under the light microscope. Ultra-thin sections were transferred to Formvar-coated slot grids (PLANO, G2500C), stained with uranyl acetate and lead citrate for 4 min each, and then examined with a JEOL JEM-1011 TEM operated at 80 kV. Digital micrographs were obtained with a mid-mount camera (MegaView III, Soft Imaging System) using iTEM imaging software (Soft Imaging System). Semi-thin sections were mounted on glass slides, stained with 1% toluidine blue in a solution of 1% sodium tetraborate (borax, modified after Richardson, Jarett, & Finke, 1960), and embedded in Roti-Histokitt II (CARL ROTH) mounting media. Light micrographs were taken with an Olympus BX60 microscope equipped with an AxioCamMRc digital camera and with an Aperio Versa 8 automatic imaging system (LEICA) including a LEICA DM6 B light microscope and an ANDOR Zyla sCMOS digital camera.

3 | RESULTS

3.1 | External morphology and tarsal distribution of tip-pore sensilla

As reported by Ganske and Uhl (2018) the number of tip-pore sensilla decreases from the tarsal tip to the femur (for the sequence of podomeres, see Figure 1b). The tip-pore sensilla are abundant on the tarsus, mostly arranged in six to eight longitudinal rows (Figure 1c,d). Tip-pore sensilla can be distinguished from other trichoid sensilla with mechanoreceptive function by their shorter length, smaller diameter and a shaft that is bent towards the tarsal claw (Figure 1c–e). The arrangement of tarsal tip-pore sensilla is similar in females

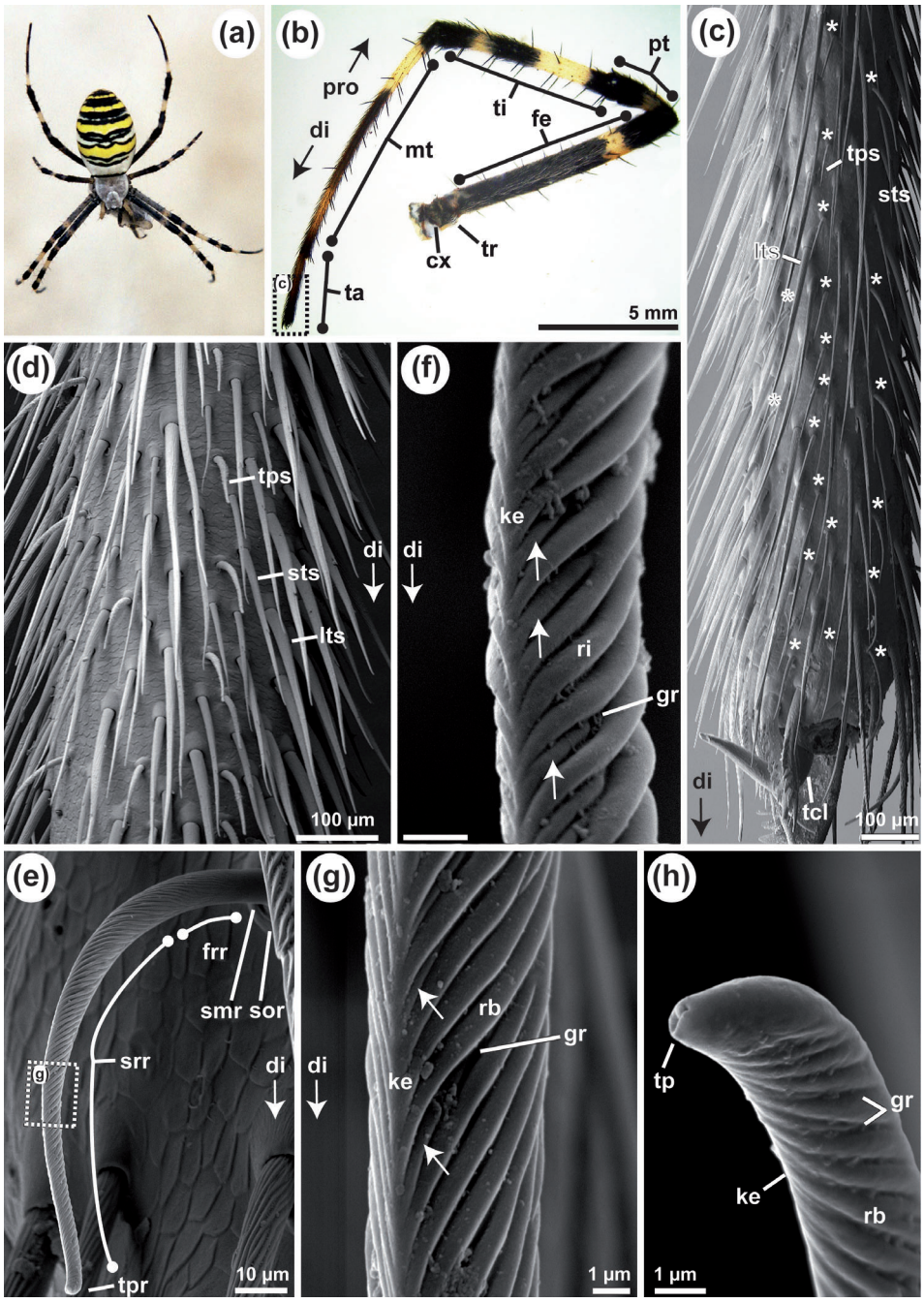

FIGURE 1 *Argiope bruennichi*, diversity of hairy protuberances found on walking legs. (a) Portrait of female individual of *A. bruennichi* from the Balearic Island Ibiza. (b) Dissected first walking leg in prolateral view showing sequence and proportions of podomeres. Micrograph. (c–h) Outer appearance of tarsal trichoid tip-pore sensilla (tps) as documented with scanning electron microscopy (SEM). (c) Overview of ventrolateral face of the tarsus bearing aligned trichoid tip-pore sensilla (asterisks); also note the presence of long (lts) and short (sts) mechanoreceptive trichoid sensilla. (d) Close up of median tarsal sector exhibiting trichoid sensilla with a strong and elongated hair shaft (lts) differing from other trichoid sensilla with shorter and slender hair shaft (sts). (e) Close-up lateral view of a tip-pore sensillum displaying five distinct regions: socket region (sor), smooth shaft region (smr), finely ribbed shaft region (frr), strongly ribbed shaft region (srr), and pore region (tpr). (f-g) Close-ups of strongly ribbed region showing upper (f) and lower (g) face of the sensillum shafts of two tarsal tip-pore sensilla in the same individual, each face tapers into a keel-like ridge (ke). Shaft surface is riddled with numerous, obliquely oriented primary ribs (rb) separated by grooves (gr). Primary ribs are interspersed by shorter and thinner secondary ribs (white arrows). Grooves and ribs show variable proportions, some tip-pore sensilla display pronounced ribs combined with broad and deep grooves (f) while others show flat and broad ribs combined with narrow, lesser deep-reaching grooves (g). The magnified sector is indicated by dashed box in (e). (h) Apical region of the shaft showing the tip pore (tp). Further labels: cx, coxa; di, distal; fe, femur; mt, metatarsus; pro, proximal; pt, patella; ta, tarsus; tcl, tarsal claw; ti, tibia; tr, trochanter [Color figure can be viewed at wileyonlinelibrary.com]

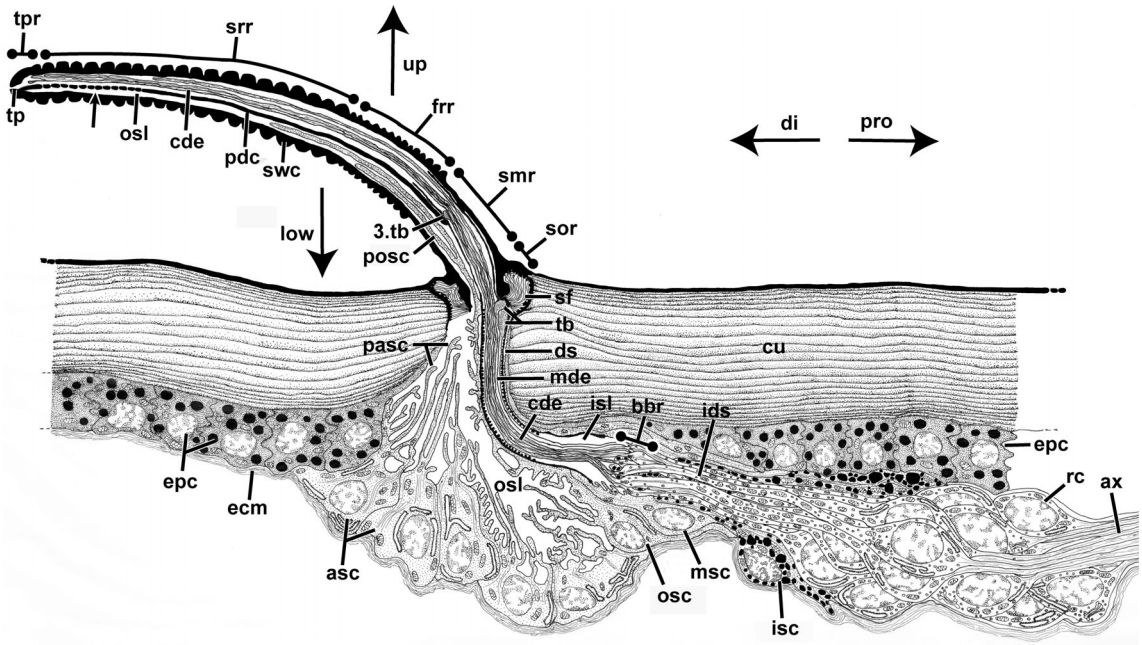

FIGURE 2 *Argiope bruennichi*, semi-schematic reconstruction of a tarsal trichoid tip-pore sensillum in longitudinal section, located on a walking leg. The sensillum shaft is bend towards the distal tip of the tarsus (di), sensillum components below the cuticle are oriented/run towards the proximal part of the tarsus (pro). Chemoreceptive dendritic outer segments (cde) and peridendritic shaft cylinder (pdc) are located in the upper domain of sensillum shaft (up) facing away from tarsal cuticle (cu), opposite lower domain (low) of sensillum shaft contains the outer sensillum lymph space (osl). Five major regions of the hair shaft can be distinguished (from distal to proximal): 1. Socket region (sor), 2. Smooth region (smr), 3. Finely ribbed region (frr), 4. Strongly ribbed region (srr), 5. Tip pore region (tpr). The arrow indicates perforated apical part of the peridendritic shaft cylinder (tubular radial projections of the outer sensillum lymph space). The longitudinal axis of the sensillum is compressed with respect to its subcuticular components, the proximal bulging of the inner sensillum lymph space (isl) is not shown in the aim to highlight the sensory components such as the dendritic inner segments (ids) and subjacent cluster of receptor cell somata (rc). We also forewent to illustrate the tiny longitudinal canals in the shaft wall cuticle. Further labels: asc, accessory sheath cells; ax, axons; bbr, basal (ciliary) body region; ds, dendritic sheath; ecm, extracellular matrix (epidermis); epc, epidermal cell(s); isc, inner sheath cell; mde, mechanoreceptive (short) dendritic outer segments; msc, median sheath cell; osc, outer sheath cell; pasc, distal projections of accessory sheath cells; posc, distal projections of inner sheath cell; sf, suspension fibres; swc, shaft wall cuticle; tb, (first and second) tubular body; 3. tb, third tubular body; tp, tip pore

and males of *A. bruennichi* and does not differ from patterns observed in both sexes of *A. blanda*. However, there is sex-specific variation in the length of the sensillum shafts. In *A. bruennichi*, shaft length varies between 80 and 150 μm in females and 70–120 μm in males. The sensillum shaft projects from the tarsal axis at a steep angle with slight variation between both sexes (50–90° in females, 40–100° in males). Five regions can be differentiated on a given sensillum shaft (Figures 1e and 2): The shaft is inserted in (1) a flat socket surrounded by a flat cuticular ring (sor, socket region), followed by a (2) region with smooth cuticular surface (Figure 5g–i) reaching up to 10 μm from the socket (smr, smooth region). In the (3) finely ribbed region (frr), the shaft is striated with frequent, narrow and flat ribs (rb) (Figure 1f–h). The cross profiles of the sensillum shaft may vary from circular to ovoid (Figure 5d–f). In the strongly ribbed region (srr) (4), along the distal half of the shaft, the ribs are fewer in number, and more pronounced. These ribs, which are called primary ribs in the following, are connected with an upper keel (facing away from tarsal cuticle) and a lower keel (facing tarsal cuticle) (ke, Figure 1f,g). The spindle-shaped cross profile is typical for this region of the shaft (Figures 3d and 5a–c). The primary ribs measure 0.47–0.65 μm in width, alternating with grooves (gr) of 0.1–0.2 μm in diameter (n = 40). The ribs vary slightly in arrangement (Figure 1f,g). Between the large primary ribs, smaller secondary ribs may be present that extend at most half way between two adjacent primary ribs (Figure 1f,g). The sensillum shaft ends at the tip-pore region (tpr) (5). The tip exhibits an ovoid pore of 0.3–0.6 μm in diameter (Figure 1h). The shaft diameter decreases from the smooth region (4–8 μm) to the tip-pore (1–2 μm).

3.2 | Internal anatomy of tip-pore sensilla

3.2.1 | General cellular organization

We found no differences in the cellular anatomy of the tip-pore sensilla on the tarsus of the first and second walking legs between female *A. bruennichi* and *A. blanda*, nor between males and females of *A. bruennichi* (Figures 3d–I and 5). Most importantly, there was no anatomical difference in tip-pore sensilla on dorsal, ventral or lateral sides of the tarsus. We document this similarity by means of cross sections

of shaft and socket structures of tarsal tip-pore sensilla from different sexes and species (Figures 5 and 6). The (sub)cellular organization of the subcuticular domain (part below the socket region) is nearly identical in both species of *Argiope*. Hence, the following descriptions and illustrations are based on ultrastructural observations in *A. bruennichi* only.

A tip-pore sensillum consists of a sensory component made of various receptor cells and a glial component consisting of various sheath cells. The sensory component is a cluster of 5 to 25 chemo- and mechanoreceptive, monociliated receptor cells located in the epidermis. Each cluster includes chemoreceptive cells (n = 2–22), which project a dendritic apparatus into the sensillum shaft. In addition,

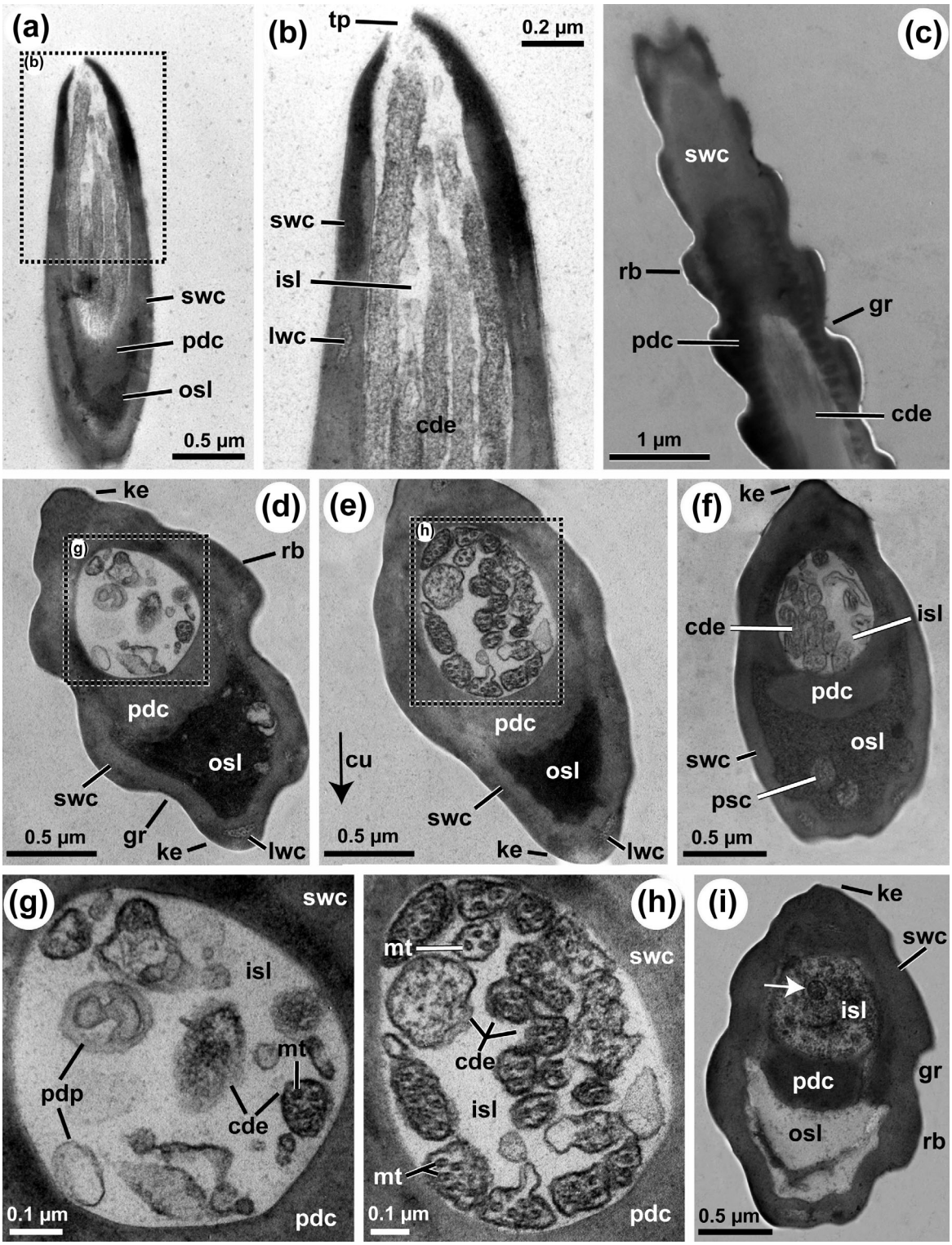

FIGURE 3 Legend on next page.

there are two to three mechanoreceptive cells that project short dendrites, which either attach to the socket (n = 1–2) or to the peridendritic shaft cylinder (n = 1). All mechanoreceptive dendrites end with a tubular body.

The following terminology of the ultrastructural components of the tip-pore sensilla is based on Keil and Steinbrecht (1984). Each dendrite is subdivided into (a) an inner segment represented by a finger-like, distal cytoplasmic process projecting from the receptor cell soma and (b) an outer segment representing the distal part of the sensory cilium, which typically lacks ciliary arrangement of microtubules (Keil & Steinbrecht, 1984). The connecting structures, namely the ciliary structure (with standard 9 × 2 pattern of microvilli) and subjacent basal bodies (bbr, basal body region; see Figure 2), comprise the ciliary region.

The glial component consists of an inner and outer sheath. The inner (main) sheath tightly surrounds the dendritic apparatus and is trifold as it is established by three overlapping sheath cells, namely the inner, median and outer sheath cell. The median sheath cell constitutes the dendritic sheath enclosing the dendritic outer segments and forms/regulates the inner sensillum lymph space (syn. "C_1 canal": Foelix & Chu-Wang, 1973a). In addition, there is an outer sheath, which is built by multiple accessory sheath cells (Figure 2). These accessory sheath cells form an epithelium below the cuticle and almost completely surround the outer sensillum lymph space (syn. "C_2 canal": Foelix & Chu-Wang, 1973a).

In the following, the cellular composition of the tip-pore sensilla is described in detail from the distal end down to the axonal strands. We thereby distinguish the supracuticular portion—the sensillum shaft including the socket—from the part where the dendritic apparatus and surrounding outer sensillum lymph space break through the thick tarsal surface cuticle, the so-called socket channel (sensu Harris, 1977), as well as the subcuticular portion, equivalent to all parts of the sensillum below the socket region and socket channel.

3.2.2 | Sensillum shaft

The sensillum shaft accommodates the chemoreceptive dendritic outer segments (cde) that project up to the tip pore region (Figure 3a,b). The width of the shaft wall cuticle (swc) continuously increases from 0.1 to 0.3 μm in the apical strongly ribbed region, over 0.3–0.5 μm in the finely ribbed region to 0.5–1.3 μm above the socket region (Figures 4–6e). The shaft wall cuticle includes a system of narrow, circularly aligned longitudinal canals (lwc) (width: 30–60 nm), which decrease in number from strongly ribbed down to the smooth region. Broad longitudinal canals have lesser electron-dense contents (Figures 3d,e, 4a,c, and 5c,f), compared to narrow longitudinal canals with extremely electron-dense lumina (Figure 5d,e). Narrow longitudinal canals can be difficult to detect in the shaft wall cuticle (Figure 5d,e). No longitudinal canal opens either to the inside or to the outside of the sensillum shaft.

The elongated chemoreceptive dendritic outer segments are situated in the upper domain of the sensillum shaft, equivalent to the upper domain of the shaft facing away from the tarsal cuticle (Figure 2). Examination of cross and oblique sections from the tip-pore region reveal that about 90% of the dendritic outer segments reach the pore (Figure 3a,b). The remaining ones seem to terminate in the strongly ribbed region (see below). The shaft regions defined in this paper are also characterized by internal ultrastructural differences. Within the strongly and finely ribbed region, the dendritic outer segments are enclosed by a cuticular cylinder, termed here as peridendritic shaft cylinder (pdc) (syn. "cuticular tube": Foelix & Chu-Wang, 1973a), which represents an involuted structure of the shaft wall cuticle. The inner portion of the peridendritic shaft cylinder separates the outer from the inner sensillum lymph space (Figures 2, 3d–f,i, 4a,c, 5a–f, and 6b,c).

Along the distal third to half of the strongly ribbed region, the inner portion of the peridendritic shaft cylinder between both lymph spaces is penetrated by radial projections (Figures 2 and 4). Longitudinal (Figures 3c and 4a,d–f), horizontal (Figure 4b), and cross (Figure 4c) sections reveal that these penetrations are tubular radial projections of the outer sensillum lymph space (osl) that almost reach the inner sensillum lymph space (isl). Only the thin, innermost lamella (intima) of the peridendritic shaft cylinder separates both lymph spaces (e.g., Figure 4c). In horizontal sections through the sensillum shaft, these tubular radial projections are cross-cut and display a

FIGURE 3 Microanatomy of tarsal trichoid tip-pore sensilla in *Argiope bruennichi* (a–h) and *Argiope blanda* (i). Distal aspect of the sensillum shaft at and immediately below the tip pore region. Transmission electron microscopy (TEM). (a,b) Cross sections of the tip pore (tp). (b) Shows details of the pore and terminals of five chemoreceptive dendritic outer segments (cde), note minute profiles of longitudinal shaft wall canals (lwc). Male. (c) Oblique-longitudinal section close-by tip pore in female. Note the slit peridendritic shaft cylinder (pdc) surrounding the chemoreceptive dendritic outer segments. (d–i) Cross sections of distalmost shaft region immediately below the tip pore and above the zone of slit circumdendritic cylinder showing considerable variation in number of chemoreceptive receptors (d,e,g,h: female of *A. bruennichi*; (f) male of *A. bruennichi*; (i) female of *A. blanda*). (d,g) Overview (d) and detail (g) of sensillar shaft housing about six chemoreceptive outer dendritic segments in the inner sensillum lymph space (isl), dendritic nature may be obscured by local swellings and subsequent rupture of microtubules (mt), only two clearly discernible dendrites are indicated in (g); (e,h) Overview (e) and detail (h) of sensillum shaft containing 20 chemoreceptive outer dendritic segments, black arrow exemplarily indicates orientation of shaft components relative to the tarsal cuticle (cu). (f) Overview of sensillum shaft containing 13 chemoreceptive outer dendritic segments. (i) Overview of sensillum shaft with only a single clearly identifiable chemoreceptive outer dendritic segment (white arrow). Note the extremely electron-dense content in the distalmost compartment of the outer sensillum lymph space (osl). Further labels: gr, grooves in shaft wall cuticle (ribbed shaft region); pdp, inward projections of the innermost lamella of the peridendritic shaft cylinder (extracellular inclusions in the inner sensillum lymph space); psc, distal cytoplasmic projections of outer and/or accessory sheath cell(s); rb, ribs on shaft wall cuticle (ribbed shaft region); ke, keel-like structure running along upper and lower edge of shaft wall cuticle; swc, shaft wall cuticle

dense and highly ordered linear pattern (Figure 4b). The lymph within these tubular radial projections appears more electron-dense towards the tip-pore region, where it can be barely distinguished from the surrounding cuticle of the peridendritic shaft cylinder (compare Figures 4d,e). A shift from moderate to high electron-density also occurs in the main compartment of the outer sensillum lymph space towards the tip-pore region (compare Figures 3d–f and 4b,d,e). Inner sensillum lymph matter was not found at the opening of the tip-pore, nor was lymph found attached to the outer surface of the sensillum shaft. The inner sensillum lymph space accommodates a varying

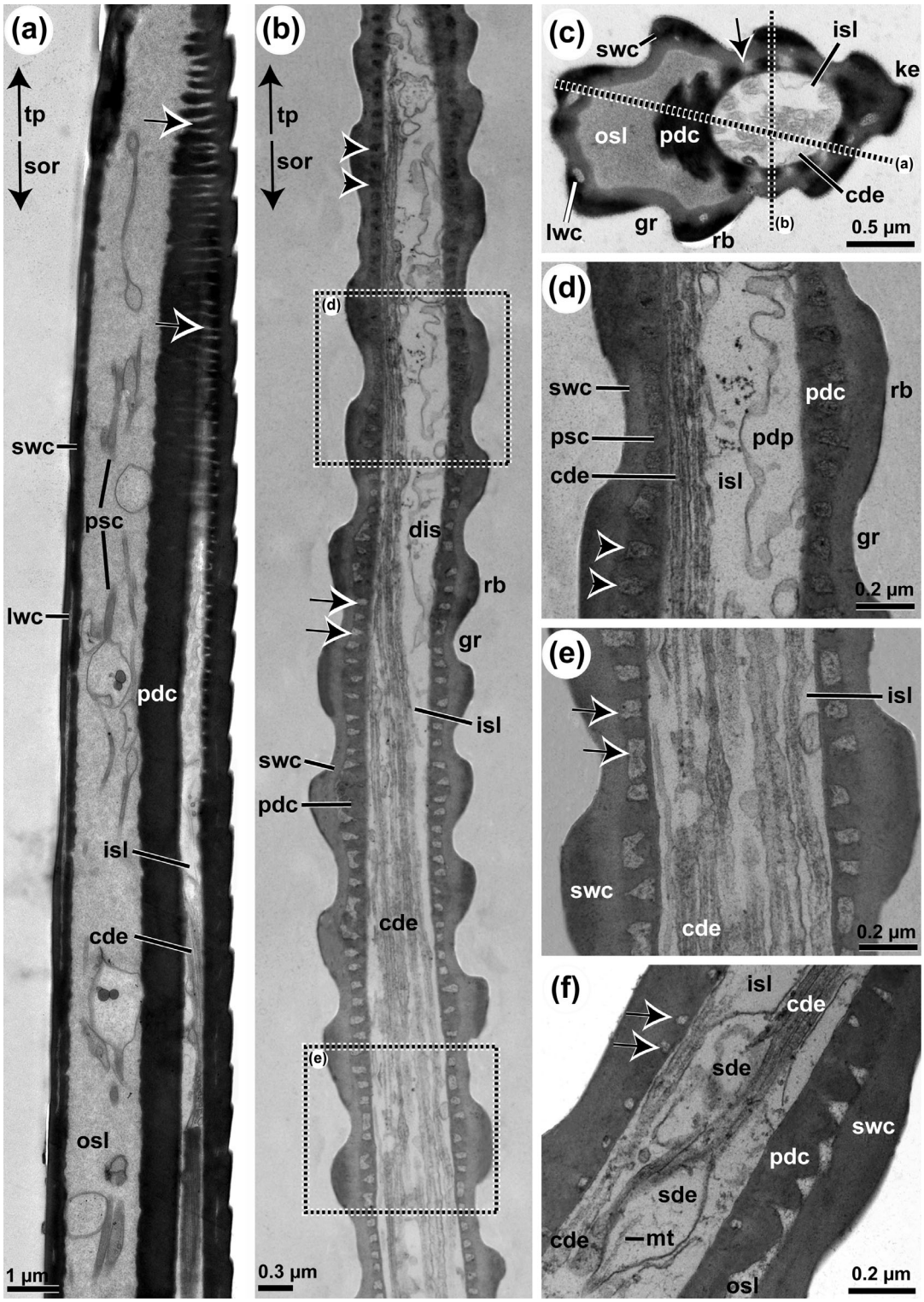

FIGURE 4 Legend on next page.

number of ramifying cytoplasmic processes (psc) formed by the accessory and/or outer sheath cell(s) (Figures 4a, 5a–h, and 6b,d–g). In the inner sensillum lymph space, we identified 2–22 chemoreceptive dendritic outer segments (cde; e.g., Figures 3d–h, 4, and 5). However, the occurrence of local swellings along some dendritic processes makes it difficult to follow individual dendrites (sde, Figure 4f) since microtubules (mt) may be locally severed and thus invisible in these regions (Figures 4f and 5d,e,g,h). Furthermore, in cross sections, local invaginations of the intima of the peridendritic shaft cylinder may resemble cellular inclusions (pdp) and may be confounded with dendritic outer segments (Figures 3g and 4d). The chemoreceptive dendritic outer segments are often restricted to a peripheral position in the inner sensillum lymph space adjoining the inner face of the peridendritic shaft cylinder (Figure 5b).

The peridendritic shaft cylinder ends at the transition of the smooth to the finely ribbed region of the sensillum (Figure 2). At this section level, the cluster of chemoreceptive dendritic outer segments is encased by a thickened dendritic sheath (ds, Figure 6a–c). Inward projections of the dendritic sheath (sds) compartmentalize the inner sensillum lymph space. One of these lymph compartments houses a small, circular tubular body (3.tb), approximately 0.2 μm in diameter, which is formed by the third mechanoreceptor cell, whereas the remaining compartments house the chemoreceptive dendritic outer segments (Figures 5g–i and 6a–c). The attachment side of the small (third) tubular body was not visible further distally (e.g., Figure 5f). The small (third) tubular body is most likely connected to the inner face and/or inward projections of the dendritic sheath (Figure 2). The dendritic sheath disappears within the peridendritic shaft cylinder further up the shaft, in the proximal half of the finely ribbed region. Here, the chemoreceptive dendritic outer segments are more dispersed within the sensillum lymph space (compare Figure 5a,f).

The sensillum shaft ends in the socket region. Here, the shaft wall cuticle is embedded in a coarsely fibrillous cuticle, here termed as suspension fibres (sf) which are part of the "joint membrane" sensu Keil and Steinbrecht (1984). The suspension fibres connect the shaft's base with the surrounding tarsal cuticle (Figures 6e,g, and 7a). In the socket region, the cluster of dendritic outer segments, enclosed by the dendritic sheath, is located at the proximal periphery (relative to the tarsus) of the outer sensillum lymph space. At the very base of the socket, usually two tubular bodies (1.tb, 2.tb) are present (Figure 2). They display a variable cross-shape and represent terminal swellings of the outer dendritic segments of the first and second mechanoreceptor cells (Figure 7). Both tubular bodies attach to the base of the shaft wall cuticle (Figure 2). In cross sections, the tubular body of the first mechanoreceptor cell is about double the size as that of the second one (Figure 7b,d,f). In approximately 10% of all tarsal tip-pore sensilla investigated, there is only a single large, ovoid tubular body (1.0–1.3 μm in diameter, Figure 7e). This tubular body most likely represents the type-1 mechanoreceptor in typical tip-pore sensilla. The tubular bodies (including the smallest third one occurring at the lower end of the peridendritic shaft cylinder) are characterized by a high abundance of microtubules, which are accurately aligned at their periphery (Figure 7d). Microtubules are embedded in a highly electron-dense matrix pervaded by interstitial filaments (Figures 6a and 7b,d–h). Peripheral microtubules (pco) contact the dendritic sheath via a complex of radiating microfilamentous spokes (Figure 7d), resembling the "membrane-integrated cones" described by Thurm et al. (1983) in insect mechanosensilla. The inner face of the dendritic sheath may show knob-like infoldings from the smooth shaft region down to the socket region (e.g., Figure 6f,h). This system of infoldings becomes more pronounced in two areas; (a) right below the peridendritic shaft cylinder (see Figure 6a–c and description above) and (b) right below the socket (Figure 7b,d,f–h). As with the transition zone to the peridendritic shaft cylinder, septum-like infoldings (sds) of the dendritic sheath separate the large tubular bodies at least partly from the chemoreceptive and the third mechanoreceptive dendrites (e.g., Figure 7d,g).

FIGURE 4 Microanatomy of tarsal trichoid tip-pore sensilla in *Argiope blanda* (a,f) and *Argiope bruennichi* (b–e, females). Distal and median aspect of sensillum shaft referred to as strongly ribbed shaft region comprising pronounced ribs (rb) separated by deep grooves (gr). Spindle-like cross profile is caused by keel-like structure lining the upper (facing away from tarsal cuticle) and lower (facing tarsal cuticle) face of the shaft (ke). Transmission electron microscopy (TEM). (a) Longitudinal section through strongly ribbed region made slightly obliquely to the shaft's medio-longitudinal axis; section plane is indicated in (c). Note the presence of slits (arrows) representing longitudinal profile of radial tubular projections of outer sensillum lymph space (osl) penetrating the peridendritic shaft cylinder (pdc), imaging of slits is enabled by cutting orientation of the cylinder changing from longitudinal (proximal, lower half of image) to tangential (distal, upper half of image). (b) Horizontal section of ribbed region almost perpendicular to a (section plane indicated in c). Stacked arrangement of numerous radial tubular projections of outer sensillum lymph space is visible (arrows and arrowheads); note the sharp gradient of electron-density in outer sensillum lymph space changing from moderate (lower half, see arrows and detail in e) to extremely high (upper half, see arrowheads and detail in d). (c) Cross section of sensilla shaft showing multiple tubular perforations in peridendritic shaft cylinder (arrow). (d) Detail of distal part of strongly ribbed shaft region in horizontal section exhibiting stacked radial projections of extremely electron-dense outer sensillum lymph space (arrowheads), note presence of chemoreceptive outer dendritic segments (cde) and inward projections of the innermost lamella of the peridendritic shaft cylinder (pdp) narrowing the inner sensillum lymph space (isl). (e) Detail of proximal part of strongly ribbed shaft region in horizontal section exhibiting stacked radial projections of moderately electron-dense outer sensillum lymph space. (f) Detail of proximal of strongly ribbed shaft region in horizontal section showing local swelling of chemoreceptive outer dendritic segments (sde); dendritic microtubules (mt) may look ripped in those swellings. Radial projections of outer sensillum lymph space are cut transversally (arrows). Further labels: lwc, longitudinal shaft wall canals; psc, distal cytoplasmic projections of outer and/or accessory sheath cell(s); sor, (direction towards) socket region; swc, shaft wall cuticle; tp, (direction towards) tip pore

3.3 | Socket channel and subcuticular portion of tip-pore sensilla

3.3.1 | General pattern

The major cytoplasmic parts of all cells constituting the tip-pore sensillum are found below the socket region (Figure 2). Here, the tarsal cuticle displays a funnel-shaped socket channel, which is traversed by the dendritic apparatus (mechano- and chemoreceptive dendritic outer segments wrapped by the dendritic sheath). The outer sensillum lymph space is lined and traversed by microvilli-form cytoplasmic processes of accessory and/or main sheath cells (psc). The dendritic apparatus stays at the proximal periphery of the socket channel (facing the side oriented towards the metatarsus). After entering the epidermis,

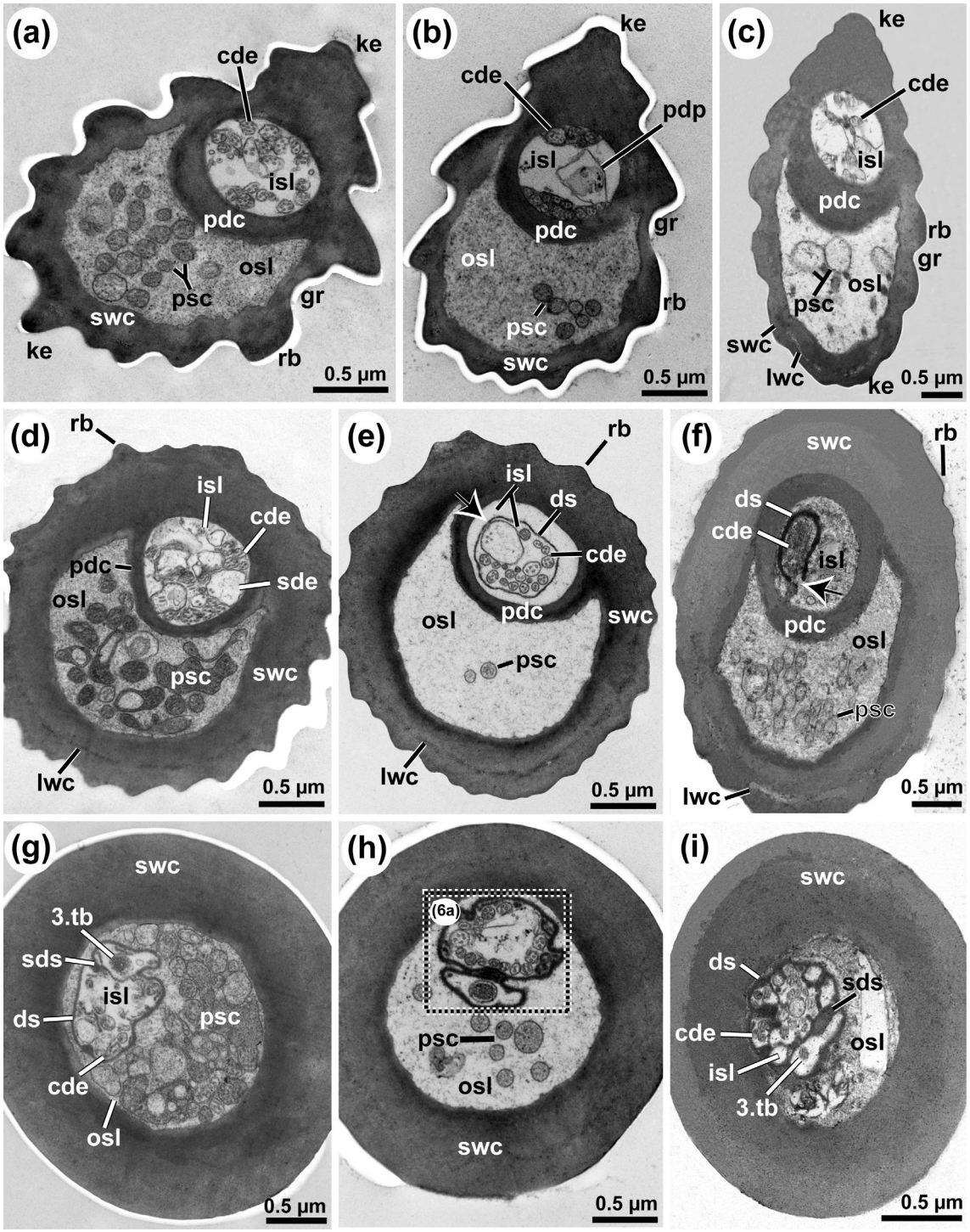

FIGURE 5 Legend on next page.

the dendritic apparatus strongly bends in proximal direction projecting up the leg towards the metatarsus at almost 90°running parallel and subjacent to the cuticle (Figures 2, 6d, and 10a).

Below the socket channel, the dendritic apparatus projects 40–50 μm through the tarsal epidermis (epc) and ends in the ciliary region indicated by the presence of ciliary structures (cis) and basal bodies (bb, bbr) (Figures 2, 7, and 10a). The distance from the ciliary region to the more proximal cluster of mechano- and chemoreceptor cell somata (rc) may vary considerably (from 20 up to 50 μm) (Figure 2). Hence, the axons of the receptor cells (ax) are usually found 60–100 μm proximally of the sensillum shaft (Figure 2). The sensory portion (receptor cell somata + dendritic processes) is tightly surrounded by multiple sheath cells and numerous, flat and granulated interstitial epidermal cells (epc) (Figure 9d). The nuclei of the interstitial epidermal cells are situated right below the socket channel (Figures 2 and 10a) or in basiepidermal position. The outer sensillum lymph space may contain granulated hemocytes (hc), which adhere to the dendritic sheath and distal processes of the outer (osc) and median (msc) sheath cells (Figure 10a,c).

3.3.2 | Receptor cells and proximal part of dendritic apparatus

Below the socket channel, the 5–25 dendritic outer segments are tightly grouped in the inner sensillum lymph space, lined by the dendritic sheath. The dendritic outer segments of the first and second mechanoreceptor cells flank the other dendrites and can be distinguished by their bigger size and lower osmiophilic cytoplasm (Figure 10b). The dendritic apparatus lies centrally in the electron-lucent outer sensillum lymph space (Figures 2 and 10a,b). The dendritic apparatus is single- or double-coated by distal processes of the main sheath cells (for more detailed description, see below). In the ciliary region, the inner sensillum lymph space is considerably wider. The dendritic sheath is formed by the median sheath cell and begins proximally at the transition zone of the median and outer sheath cell (Figures 2, 8a, and 10a). The dendritic outer segments turn into ciliary segments (cis) in the widened proximal part of the inner sensillum lymph space not covered by the dendritic sheath, where they form the ciliary segment (cis). Here, each ciliary segment possesses a standard 9×2 ciliary configuration of microtubules (Figures 8b–d and 10a). At the basal rim of the widened part of the inner sensillum lymph space, each ciliary segment is connected to two, linearly arranged centromers forming the region of the basal body (bbr) and located at the tip of the finger-like dendritic inner segment (ids, Figures 2 and 8b,d). The horizontal arrangement of inner dendritic segments across this area is caused by the row-by-row descent of the ciliary segments towards the bottom of the inner sensillum lymph space. Ciliary segments turn into dendritic inner segments at the region of the basal body (bbr). Dendritic inner segments form a flat bundle that projects further proximally, crammed between the inner and median sheath cell (Figures 8c–e and 9b). The cytoplasm of the inner dendritic segments contains a complex system of elongated, partly branched mitochondria of the cristae type (mi), dispersed cisternae of the rough endoplasmic reticulum (rER), longitudinally running microtubules, small electron-lucent vesicles (ev) located around the basal body, as well as ciliary root filaments (cr) projecting from the basal body (Figures 2 and 8b–e). We did not find any differences between the dendritic inner segments and, thus, could not differentiate between chemo- and mechanoreceptor cells in this part of the sensillum. In the soma region, dendritic inner segments widen into a spherical to ovoid compartment (soma) carrying the circular nucleus (nu) with poor heterochromatin content (Figure 9a,c). The perinuclear cytoplasm of the receptor cells is moderately electron-dense and includes elongated mitochondria (cristae type), highly ordered cisternae of the rER, Golgi stacks (go), numerous coated vesicles, vacuoles with contents of heterogenous electron-density resembling lysosomes, and dispersed microtubules (some of listed organelles illustrated on Figure 9c). Proximally, each receptor cell soma tapers into a long axonal process containing slender and elongated mitochondria and microtubules. The 2–25 axons of a given tip-pore sensillum form a distinct axon bundle projecting proximally. Further up the tarsus, axon bundles of neighbouring tip-pore sensilla merge to form joint, second-order axon bundles (axb) (Figure 9d).

FIGURE 5 Comparative morphology of trichoid tip-pore sensilla in *Argiope* spp. Compilation of cross sections demonstrating highly similar architecture of sensillum shafts as depicted from various section levels. (a,d,g) *Argiope bruennichi*, female; (b,e,h) *Argiope bruennichi*, male; (c,f,i) *Argiope blanda*, female. Transmission electron microscopy (TEM). (a–c) Proximal aspect of strongly ribbed shaft region, below zone of pierced peridendritic shaft cylinder (pdc). Note varying numbers of chemoreceptive outer dendritic segments (cde: a: 20, b: 16, c: 14) and distal cytoplasmic projections of various sheath cells (psc: a: 17, b: 6, c: 3). (b) Shows typical central position of locally invaginated innermost lamella of the peridendritic shaft cylinder (pdp) squeezing the chemoreceptive dendritic outer segments into a peripheral position within inner sensillum lymph space (isl). (d–f) Spherical to ovoid cross profiles of sensillum shafts found in finely ribbed shaft region: (d) Amidst finely ribbed region with chemoreceptive dendritic outer segments dispersed in inner sensillum lymph space, note the presence of swollen dendrites (sde). (e) Proximal aspect of finely ribbed shaft region; inner sensillum lymph space occurs in two distinct compartments separated by the dendritic sheath (ds); one chemoreceptive outer segment appears swollen (arrow). (f) Section level a few micrometres distal to (e) identifiable by disintegration of the dendritic sheath (arrow). (g–i) Spherical cross profiles of smooth region near-by base of sensillum shaft. All sections show a small tubular body (3. tb) representing the termination structure of the shaft-invading, third mechanoreceptor cell which is separated from chemoreceptive dendrites by septum (sds) formed by heavily diversified dendritic sheath. The peridendritic shaft cylinder is absent in this region. Detail of dendritic apparatus shown in h is given in Figure 6a. Further labels: gr, grooves in shaft wall cuticle (ribbed shaft region); lwc, longitudinal shaft wall canals; osl, outer sensillum lymph space; psc, distal cytoplasmic projections of outer and/or accessory sheath cell(s); rb, ribs on shaft wall cuticle (ribbed shaft region); ke, keel-like structure running along upper and lower edge of shaft wall cuticle; swc, shaft wall cuticle

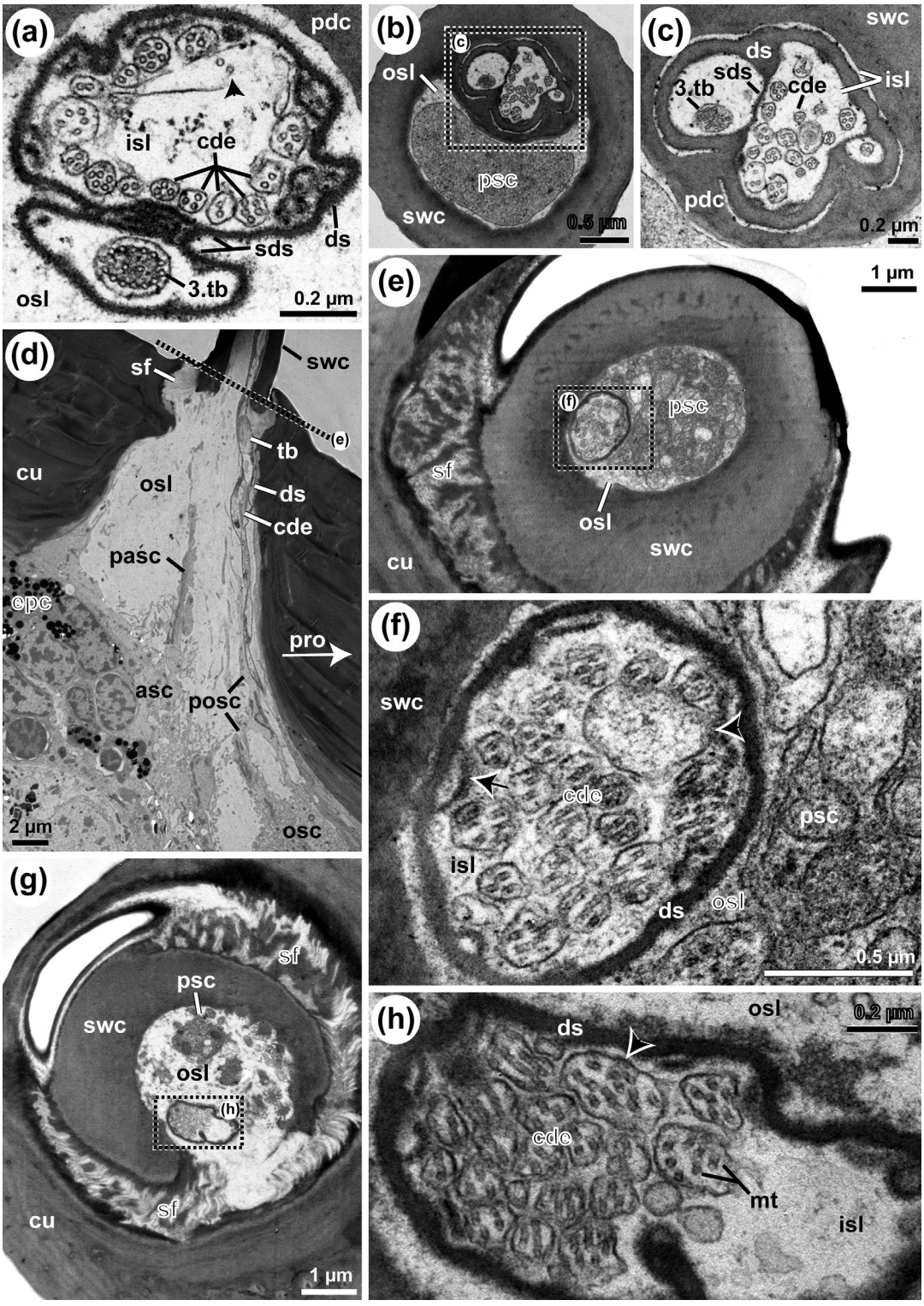

FIGURE 6 Legend on next page.

3.3.3 | Sheath cell system

The sheath cell system of tip-pore sensilla in *A. bruennichi* and *A. blanda* is established by both main and accessory sheath cells. The main sheath cells constitute the main (inner) sheath by surrounding the receptor cells including the dendritic apparatus and the inner sensillum lymph space. The accessory sheath cells do not have direct contact with the sensory system but establish a second (accessory) sheath as they line the outer sensillum lymph space. The main sheath is formed up by three stacked cells each of which is represented by a distinct type of sheath cell, defined by its position, cytoplasmic composition, apical differentiation, and function. Inner, median, and outer sheath cells can be distinguished.

The inner sheath cell (isc) surrounds the most proximal and spacious part of the inner sensillum lymph space, which is not lined by a dendritic sheath. This area is termed "basal lymph cavity" in insect tip-pore sensilla (Ozaki & Tominaga, 1999). The proximal part of the apex of the inner sheath cell projects numerous slender and elongated microvilli (mv), which invade this proximal lumen of the inner sensillum lymph space (Figures 8a–c and 9a,b). Further characteristics of this cell type are elongated mitochondria (cristae type) in the cytoplasm, a massively developed rER, numerous and slightly polymorphic granules (g) with extremely electron-dense content and measuring up to 3 μm in diameter, membrane-enclosed vacuoles with a heterogenous matrix resembling lysosomes, few Golgi stacks, as well as dispersed microtubules (Figure 10a,d,e). The soma of the inner sheath cell is usually located at the proximal end of the inner sensillum lymph space. The nucleus is ovoid or bean-shaped and contains moderate portions of heterochromatin (Figure 10a,d,e).

The median sheath cell (msc) surrounds the entire apex of the inner sheath cell (Figures 2, 9a,b, and 10a) and, slightly further distally, also the inner sensillum lymph space at the level of the basal body region and the ciliary segment (Figures 8a,c,e, 9a, and 10a). The median sheath cell transforms into a thin ring enclosing the dendritic apparatus and the inner sheath cell to which it is connected by septate junctions (sj, Figure 9b). The median sheath cell is equipped with an extensive system of microtubules. At the transition to the outer sheath cell, the median sheath cell secretes the dendritic sheath (e.g., Figures 8a and 10a). Along the entire overlapping zone, the ring is encompassed peripherally by a second (outer) ring formed by the outer sheath cell (Figures 2, 8a, and 10a). Distally, at the level of the outer sensillum lymph space, the (inner) ring tapers off into numerous, elongated, and often ramified microvilliform processes including numerous microtubules. These distal processes enter the outer sensillum lymph space and may run in the vicinity of the dendritic sheath (e.g., Figures 2 and 10a,b). Some of them extend up to the socket region (Figures 2 and 6d). The soma of the median sheath cell is mostly found basally of the inner sensillum lymph space, approximately 10 μm proximally of the ciliary segment. The cytoplasmic composition of the median sheath cell is similar to that described for the inner sheath cell, but it lacks the polymorphic, highly electron-dense granules.

The third main sheath cell, the outer sheath cell (osc), locally overlaps with the median one (e.g., Figure 2). It has no direct contact with the inner sensillum lymph space, it surrounds the dendritic sheath and, more proximally, also the (inner) ring formed by the median sheath cell (Figures 2, 8, 9b, and 10a). The (outer) ring formed by the outer sheath cell along the overlapping zone with the median sheath cell reaches farer distally than the inner ring. The (outer) ring is often punctuated by the distal microvilliform processes of the median sheath cell along the entire subcuticular portion of the dendritic apparatus. Where the main sheath has separated from the dendritic sheath, the elongated distal processes of the outer sheath cell continue along the dendritic sheath into the cuticular breakthrough area, the socket channel (Figures 2 and 6d). Along their pathway, they overlay the dendritic sheath and are subjacent to the cuticle (compare

FIGURE 6 Microanatomy of tarsal trichoid tip-pore sensilla in *Argiope bruennichi* (a–c: males, e–h: females) and *Argiope blanda* (d). Proximal aspect of sensillum shaft (smooth region, a–c) as well as sections from socket region down the socket channel showing profiles of the dendritic apparatus (d–h) in cross (a–c, e–h) and longitudinal (d) sections. Transmission electron microscopy (TEM). (a) Detail of 15 chemoreceptive dendritic outer segments (cde) in ring-like formation separated from small tubular body (3.tb) which represents the termination structure of the shaft-invading, third mechanoreceptor cell. One chemoreceptive dendrite appears swollen and deformed but is still identifiable by its microtubules (arrowhead). Sector marked on Figure 5h. (b,c) Transition zone of smooth and finely ribbed shaft region indicated by overlapping of thickened dendritic sheath (ds) and proximal tip of the peridendritic shaft cylinder (pdc): (b) Overview. (c) Detail of dendritic apparatus (sector marked in b). Section level is situated between those illustrated in Figure 5d–f,g–i. The small tubular body is still present and separated from the remaining chemoreceptive dendritic outer segments by septal infolding of the dendritic sheath (sds). (d) Overview of socket region and subjacent passage of dendritic apparatus through socket channel; dendritic outer segments are restricted to proximal rim of inflated outer sensillum lymph space (osl) which is traversed by ramified distal projections of the accessory (pasc) as well as of outer sheath cell (posc). (e,f) Distal aspect of socket region: (e) Overview, flexible suspension fibres (sf) are observed around half of the base of the shaft wall cuticle (swc), outer sensillum lymph space is endowed with distal projections of sheath cells, section orientation indicated in (d); (f) Detail of the dendritic apparatus, 21 outer dendritic segments are visible, presumed third mechanoreceptive dendritic outer segment is marked by an arrowhead, knob-like infoldings of the dendritic sheath are exemplarily indicated by arrow. (g,h) Median aspect of socket region: (g) Overview, suspension fibres are attached to nearly all sites of proximal tip of shaft wall cuticle which is not present anymore at lower right due to slightly oblique section orientation; (h) Detail of dendritic apparatus comprising 19 dendritic outer segments (not the same sensillum as shown in e!), the presumed third mechanoreceptive dendritic outer segment is marked by an arrowhead. Further labels: asc, accessory sheath cells; cu, tarsal cuticle; epc, epidermal cells; isl, inner sensillum lymph space; mt, dendritic microtubules; osc, outer sheath cell; psc, distal cytoplasmic projections of outer and/or accessory sheath cell(s); tb, tubular body of first or second mechanoreceptor cell

Figure 10b), whereas the lower surface of the dendritic sheath, which faces the epidermal extracellular matrix, is not covered (Figure 10b). Further distally, the distal processes separate from the dendritic sheath and ramify. Some of these distal ramifications pass through the socket region (Figures 2 and 6d,g) and extend up to the strongly ribbed region of the sensillum shaft (Figures 2 and 5; posc). The soma

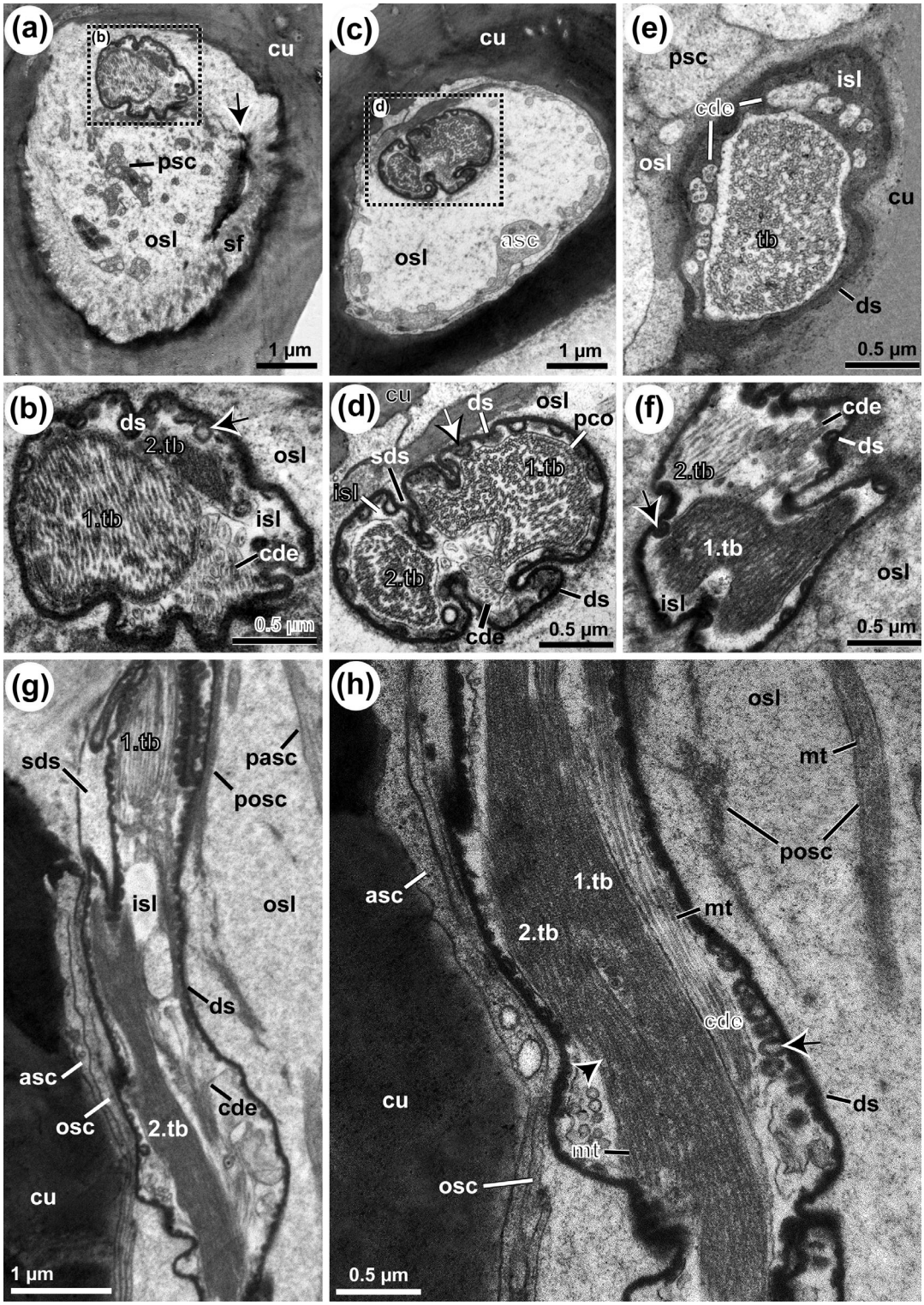

FIGURE 7 Legend on next page.

of the distal sheath cell is usually found adjacent to the soma of the median sheath cell (Figure 2). The appearance of the nucleus and the composition of the cytoplasm of the outer sheath cell are similar to that of the median sheath cell.

Accessory sheath cells (asc) line the largest (lateral and basal) parts of the outer sensillum lymph space in the area below the cuticle and within the socket channel. 5–12 accessory sheath cells are found in an epithelium-like arrangement. The cytoplasmic protrusions of the most distal accessory sheath cells (as to the leg longitudinal axis) project towards the socket region (e.g., Figures 2 and 6d) and may also invade the sensillum shaft, where they display unbranched, microvilliform tubes (pasc) which are hardly distinguishable from the shaft-invading processes of the outer sheath cell (e.g., Figure 5). More proximally located accessory sheath cells, however, may also project true microvilli into the outer sensillum lymph space (Figure 10a,c). The tip of the microvilli shows an electron-dense plaque (Figure 10c), which may connect to microfibrils projecting deeper into the lymph space. These microfibrils seem to make contact with the dendritic sheath (not illustrated). The cytoplasm of the accessory sheath cells is highly electron-dense and mainly contains membrane-bordered vacuoles of various shapes and sizes (up to 4 μm in diameter). These vacuoles appear empty (eva) or filled with numerous spherules of varying electron-density. The vacuoles, which are fully occupied by these spherules, resemble multivesicular bodies (lys) that represent an early stage in the lysosomal transformation cascade (Figure 10d). We also found few small, elongated mitochondria (cristae type), dispersed or locally stacked rough ER cisternae, and polyribosomes. The ovoid nucleus is located at the base of the cell and contains a moderate portion of heterochromatin (Figure 10d).

3.3.4 | Other types of trichoid sensilla (cellular anatomy not illustrated)

TEM also provides additional information on the internal cellular organization of other trichoid sensilla. All trichoid sensilla on the tarsus of the first and second walking legs of *A. bruennichi* and *A. blanda* show close resemblance with "tactile hair sensilla" (sensu Foelix & Chu-Wang, 1973b) despite differences in size and socket elevation (Figure 1d). Their sensillum shafts have a thick wall cuticle, carry a narrow central lumen devoid of any dendrites, and lack a terminal pore. Three large tubular bodies attach to the proximolateral face of the shaft wall cuticle. Each tubular body is the mechanoreceptive terminal of a slim dendritic outer segment projected by a single (monociliated) receptor cell. There are no dendrites projecting into the sensillum shaft. The surrounding sheath cell system (three main—inner, median, outer—sheath cells + multiple, epithelially arranged accessory sheath cells), arrangement of inner and outer sensillum lymph spaces, and subcuticular projection pathways of dendritic outer segments closely resemble the pattern found in the tip-pore sensilla.

4 | DISCUSSION

4.1 | Comparative morphology of tip-pore sensilla in spiders

4.1.1 | General remarks

The present TEM study explored the outer and the inner ultrastructure of tip-pore sensilla on the tarsus of the first two walking legs of *A. bruennichi* and *A. blanda*. The tip-pore sensilla are bimodal sensory systems mostly comprising three mechanoreceptive cells as well as 2–22 chemoreceptive cells. The elongated dendrites of the chemoreceptive cells project through the peridendritic shaft cylinder and terminate at the tip-pore. Along the entire length of the shaft, except for the terminal pore, there are no wall pores in the shaft wall cuticle. We found a previously undetected third mechanoreceptive cell, which connects to the proximal end of the peridendritic shaft cylinder by a small tubular body. In contrast, the dendrites of the already known first and second mechanoreceptive cell terminate at the socket.

Our TEM data show that the sensillum shaft of *A. bruennichi* and *A. blanda* can vary in length, amount of curvature, and surface morphology as well as in the number and ultrastructural organization of receptor cells and associated dendrites. With the exception of some tip-pore sensilla with less than 10 or more than 20 chemoreceptive cells included, the number of chemoreceptive cells usually varies from 10–18 in the tarsal tip-pore sensilla of both *Argiope* species. The

FIGURE 7 Microanatomy of tarsal trichoid tip-pore sensilla in *Argiope bruennichi* (a–c,e: males, c,d: females) and *Argiope blanda* (f–h). Details of socket channel with special focus on area immediately below socket region highlighting first one to two mechanoreceptive dendrites terminating in large tubular bodies attaching to base of shaft wall cuticle and suspension fibres. Transmission electron microscopy (TEM). (a–f) Various cross sections (a,c: overview, b,d–f: detail of dendritic apparatus) showing close intra- and interspecific similarity in arrangement of the usually two tubular bodies (1.tb, 2.tb) in comparison to the cluster of the much smaller chemoreceptive dendritic outer segments (cde) (a–d,f). The occasionally encountered variant with only one tubular body attaching to shaft base is illustrated in (e). Note the multiple infoldings of the dendritic sheath (ds), built either by its innermost lamella (see arrows in b,d,f) or the entire sheath resulting in septum-like partition (sds) of tubular bodies and chemoreceptive dendritic outer segments. Basal remains of shaft wall cuticle (arrow) including associated suspension fibres (sf) shown in a indicates closest vicinity to socket region. (g,h) Details of tubular bodies of first and second mechanoreceptors in longitudinal section, note the highly electron-dense protein matrix (see arrowhead in h) filling the interstices of highly ordered and condensed microtubules (mt). Arrow in h points at bulbs of the innermost lamella of the dendritic sheath folding into the inner sensillum lymph space (isl). Cytoplasmic processes of accessory (asc) and outer (osc) sheath cells interdigitate at the periphery. Further labels: cu, tarsal cuticle; osl, outer sensillum lymph space; pasc, distal projections of accessory sheath cells; pco, complex of peripherally aligned microtubules and membrane-integrated cones; posc, distal cytoplasmic projections of outer sheath cell; psc, distal cytoplasmic projections of outer and/or accessory sheath cell(s)

number of chemoreceptive cells in the tip-pore sensilla of arachnids is generally high (e.g., Foelix, 1985) compared to insects, which usually possess four chemoreceptive cells per sensillum (review of Ozaki & Tominaga (1999)). The number of chemoreceptive cells might diversify the realized reaction spectrum (Harris & Mill, 1977) and might allow detecting different chemical compounds with different cells

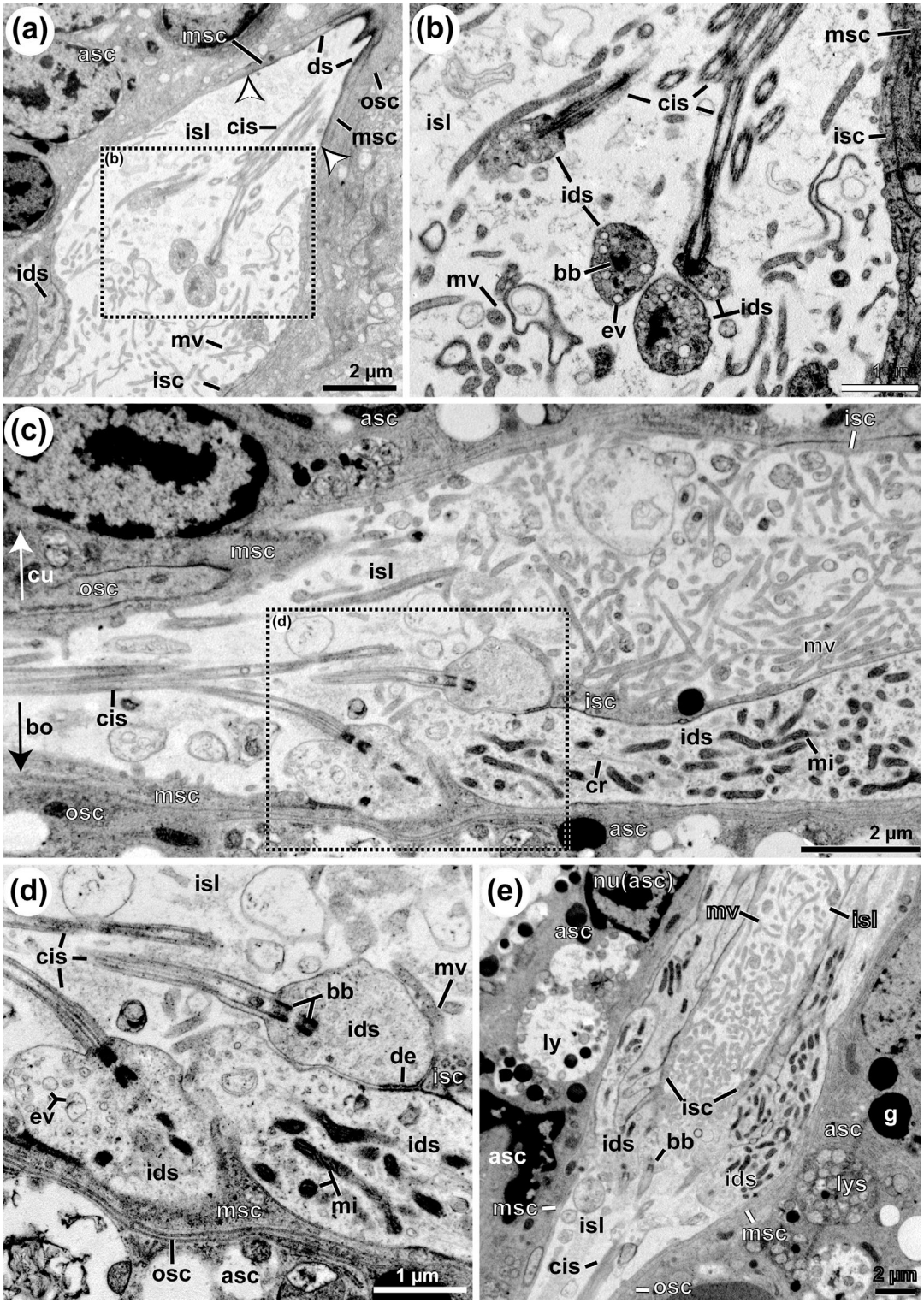

FIGURE 8 Legend on next page.

within one sensillum (Tichy et al., 2001). Alternatively, fine-scale detection of odours may be achieved by encoding the quality and concentration of particular compounds as the pattern of excitation across the array of chemoreceptive cells (Erickson, 1963; Tichy et al., 2001). Either way, the complexity of chemoreception, namely by differential perception of odours, may be enhanced if the number of chemoreceptive cells is increased. Since the number of chemoreceptive cells was not related to specific areas and orientation on the tarsus, we have no indication of regional morphological differences that might correspond to functional differences; the tip-pore sensilla facing away from the substrate did not differ in shape and composition from those that contact the substrate.

4.1.2 | Structural correspondences in tip-pore sensilla of spiders

Tip-pore sensilla have been studied previously in seven species of entelegyne araneomorph spiders and, in lesser anatomical detail, three species of mygalomorph tarantula spiders. An overview of the various (sub-)cellular components of tarsal tip-pore sensilla across hitherto studied spider species is given in Table 1, a more exhaustive compilation can be taken from supplementary online material Table S1, which includes more information on the morphometry as well as the outer and inner ultrastructure of the sensillum shaft. Tip-pore sensilla of the so far studied spider species have the following microanatomical features in common: (1) located on walking legs and pedipalps, (2) slightly bent or S-shaped, ribbed or spinose sensillum shafts projecting from the cuticle at a steep angle (measuring 40–100° from cuticular surface), (3) a thin shaft wall cuticle surrounding a voluminous central lumen, and (4) a single subterminal pore. More shared characters concerning the inner anatomy of the sensillum shaft are: (5) a peridendritic shaft cylinder, which surrounds the dendritic outer segments along almost the entire length of the sensillum shaft, (6) longitudinal canals in the shaft wall cuticle, and (7) a usually thin dendritic sheath surrounding the dendritic outer segments up to the peridendritic shaft cylinder. This sheath separates the dendritic outer segments by forming infoldings at the level of the tubular bodies, and does not connect to the sensillum shaft's base.

Shared characters of the sensory apparatus are (8) a maximum of 18 monociliated, unbranched chemoreceptive cells projecting their outer dendritic segments towards the sensillum shaft and (9) usually two large mechanoreceptive cells, whose tubular bodies attach to the base of the sensillum shaft (socket region). Common characters of the sheath cell system are (10) four cell types: inner sheath cell, median sheath cell, and outer sheath cell that build the inner sheath, which surrounds the dendritic apparatus. The outer (accessory) sheath is formed by several accessory sheath cells forming an elaborate system of microvilli. Furthermore, the sheath cell system surrounds and forms two sensillum lymph spaces (11). The inner lymph space accommodates the dendritic apparatus (wrapped by the main sheath), while the outer lymph space is lined by the epithelium of accessory sheath cells.

4.1.3 | Unique characters of tip-pore sensilla in Araneidae

Some ultrastructural characters of the tip-pore sensilla on the leg tarsus of the so far investigated species *Argiope* spp. (this paper) and *Araneus diadematus* Clerck, 1757 (Foelix, 1970; Foelix & Chu-Wang,-1973a) are either novel or the result of reassessment (Table 1). Novel characters of tip-pore sensilla of *Argiope* spp. are (a) the stacked radial canals in the peridendritic shaft cylinder, (b) a third mechanoreceptive cell terminating with a small tubular body attached to the proximal end of the peridendritic shaft cylinder, (c) the compartmentalization of and steep concentration gradient within the outer sensillum lymph space close-by the tip pore, and (d) the complex epithelial arrangement of accessory sheath cells (Table 1).

The reassessment of ultrastructural data provided by Foelix (1970) and Foelix & Chu-Wang (1973a) suggests that tip-pore sensilla of *A. diadematus* also share most of the characters listed above (1–2 and 4). For instance, Figure 10 in the paper by Foelix & Chu-Wang (1973a) reveals a serrated inner wall of the peridendritic shaft cylinder. The same authors also present a cross section of the sensillum shaft below the tip pore showing a radial process of the outer sensillum lymph

FIGURE 8 *Argiope bruennichi*, microanatomy of tarsal trichoid tip-pore sensilla (a,b: females, c–e: males) as depicted from horizontal (a,b,e) and longitudinal (c,d) sections. Subcuticular portion: transition zone (= ciliary region) of inner (ids) and outer dendritic segments identifiable by the ciliary segment (cis) connected to the basal bodies (bb). Transmission electron microscopy (TEM). (a,b) Section through voluminous, disk-shaped inner sensillum lymph space (isl) massively crossed by microvilli (mv) projected by inner sheath cell (isc): (a) Overview horizontal section, close-by and parallel to bottom (bo) of the inner sensillum lymph space; inner sensillum lymph space is only lined by dendritic sheath (ds) distal to ciliary region; white arrowheads mark proximal end of the dendritic sheath. (b) Detail of basal bodies of four dendrites in both cross and longitudinal section. (c,d) Complementary section perpendicular to section orientation shown in (a and b): (c) Overview, three dendritic inner segments are cut along their longitudinal axis, running along the bottom (bo) of the inner sensillum lymph space (basal end facing away from tarsal cuticle). (d) Detail of the distal tip of the three dendritic inner segments shown in (c) (dashed box); note the presence of stacked, equally oriented basal bodies in the basal (ciliary) body region, cytoplasm is rich in branched mitochondria (mi). (e) Horizontal section through bottom of inner sensillum lymph space approximately 5 μm below section level shown in (a). Many dendrites are visible at the level of their outer dendritic segment, ciliary region and, predominantly, of closely adjoined inner dendritic segments. Dendrites as well as profiles of the outer and median sheath cells (osc, msc) are wrapped by numerous accessory sheath cells (asc) containing lysosomes of different age (lys) as well as extremely electron-dense granules (g). Further labels: cr, ciliary rootlet; cu, tarsal cuticle; de, desmosome (zonula adhaerens); ev, electron-lucent vesicle(s); nu(asc), nucleus of an accessory sheath cell

space that extends into the interspace of the shaft wall and the peridendritic shaft cylinder (Foelix & Chu-Wang, 1973a). This cross section moreover shows an extracellular inclusion in the cylinder displaying the same electron-density as the lymph space (see their Figure 13). Therefore, we find it likely that radial canals are also present in the peridendritic shaft cylinder of tip-pore sensilla in

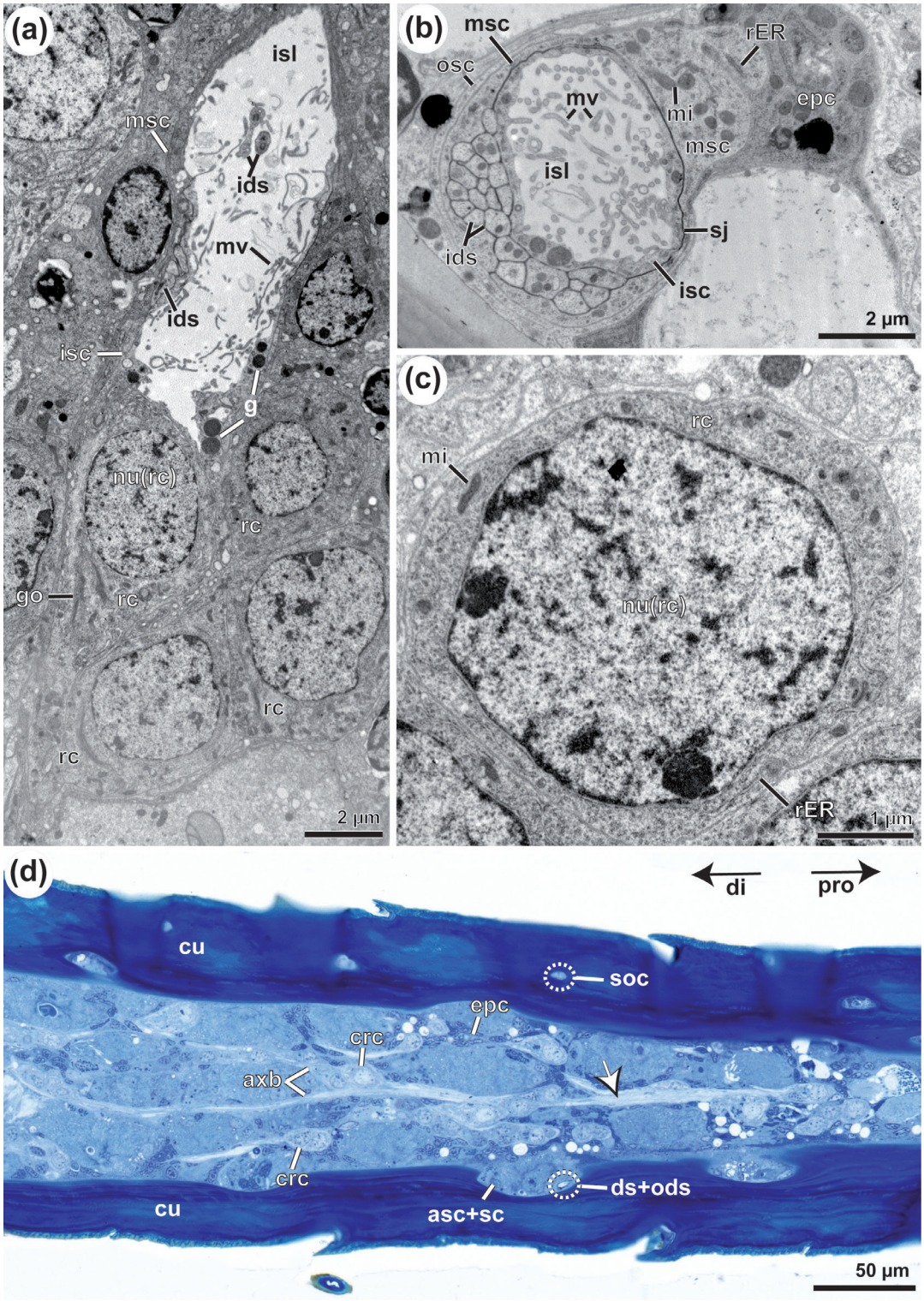

FIGURE 9 Legend on next page.

A. diadematus. The radial canals might have been overlooked due to unfavourable section planes. Further, Foelix & Chu-Wang (1973a) sectioned but did not describe a third small tubular body (compare their Figure 11 with Figure 6b,c in the present paper). These ultrastructural similarities suggest that at least Characters 1 (radial canals in the shaft cylinder) and 2 (a third mechanoreceptive cell) as listed above are shared traits of orb-weaving spiders (Araneidae). Whether Characters 3 and 4 are also present in araneid spiders other than *Argiope* requires further investigation.

4.2 | Bimodality of tip-pore sensilla: Chemoreceptors and mechanoreceptors combined

4.2.1 | Chemoreceptors

The trichoid tip-pore sensilla of *Argiope* are characterized as bimodal receptors for chemoreception and mechanoreception, a widespread combination among both terrestrial and aquatic arthropods (Arachnida: e.g., Foelix & Chu-Wang, 1973a; Foelix, 1985, 2011; Myriapoda: Müller, Sombke, Hilken, & Rosenberg, 2011; Müller & Sombke, 2015; Crustacea: e.g., Hallberg & Skog, 2011; Hexapoda: e.g., Zacharuk, 1980; Ozaki & Tominaga, 1999; see also general review of Altner & Prillinger (1980)). Since the tip-pore sensilla of *Argiope* and other araneomoph or mygalomorph spiders contain multiple receptor cells that project up to the single terminal pore of an otherwise pore-less sensillum shaft, it is assumed that the terminal pore is the only possible passageway for chemical information. Such tip-pore sensilla resemble strongly those chemoreceptors of insects that are used for contact-chemoreception.

We consider the peridendritic shaft cylinder of the tarsal tip-pore sensilla of *Argiope* spp. as a feature supporting contact-chemoreception. It might shield the dendritic receptors from getting in contact with stimulating molecules along their entire length in the shaft except for the tip-pore region. Based on the concept of Morita (1992), which addresses the specific role of the dendritic and other cuticular sheaths in maintaining the bioelectric circuit within the sensillum shaft (syn. "depolarizing current": Rees, 1967), the dendritic sheath and peridendritic shaft cylinder combined may act in combination as an effective insulator. The breakthroughs in the distal part of the peridendritic shaft cylinder may also play a crucial role in completing the electric circuit (see Ozaki & Tominaga, 1999, figure 2) as these radial canals provide the only places, where the outer and inner sensillum lymph spaces come in close contact to each other.

In our study, some dendritic outer segments showed swellings, membrane disruptions (especially nearby the terminal pore), myelin-like structures, and only few dispersed, locally disconnected microtubules. These damages are possibly caused by aldehydes included in the primary fixative. Similar damages were repeatedly found at the tips of the dendritic outer segments of gustatory receptor cells in labellar tip-pore sensilla of the blowfly *Phormia regina* Meigen, 1826. Both TEM observations and electrophysiological recordings showed that the terminals of gustatory dendrites are damaged when exposed to harmful substances, such as the detergent deoxycholate (DOC) (Ninomiya, Ozaki, Kashihara, & Morita, 1986; Ozaki, Ninomiya, Kashihara, & Morita, 1986; Ozaki & Tominaga, 1999). As with tarsal tip-pore sensilla of *Argiope* spp., we therefore assume that at least those receptor cells with damaged terminals may serve gustation, while the other dendritic outer segments, which stayed intact during fixation, may rather serve olfaction.

The finding that the tarsal tip-pore sensilla of *Argiope* spp. are similar to those of insect contact receptors raised the question as to whether and how spiders can perceive volatile substances. As hypothesized above, some chemoreceptive dendritic outer segments might be specialized in responding to olfactory cues rather than to soluble contact stimuli. However, gustation and olfaction should be considered "two extremes of a continuum" (Stengl, 2019). In most arthropods, the contact-chemoreceptive tip-pore sensilla and olfactory wall-pore sensilla are distinguished by means of many factors, such as the location of the sensillum, responses at lower (long-distance detection of volatile odours) or higher (short-distance detection of soluble or substrate-bound odours) stimulus thresholds, as well as receptor types and their specific physiology. Further differences concern functional ultrastructures in and immediately below the sensillum shaft, mechanisms of stimulus transduction, and projection patterns in the central nervous system (e.g., Ozaki & Tominaga, 1999; Stengl, 2019; Stocker, 1994; Zacharuk, 1980). Contact-chemoreceptors of pterygote insects are well understood and, therefore, are used in the following for comparison with the available knowledge on araneid spiders.

FIGURE 9 *Argiope bruennichi*, microanatomy of tarsal trichoid tip-pore sensilla (a–c: females, d: male) as depicted from horizontal (a,d) and cross (b,c) sections. Subcuticular portion: proximal part of sensillum around zone of receptor cell somata. (a–c): Transmission electron microscopy (TEM), (d): Light microscopy. (a) Horizontal section near bottom of inner sensillum lymph space (isl) similar to section plane visible in Figure 8a, exhibiting several profiles of dendritic inner segments (ids) as well as several receptor cell somata (rc) including Golgi stacks (go). (b) Cross section of dendritic apparatus at the level of dendritic inner segments, 21 are visible lining the bottom of the inner sensillum lymph space; note triple-fold wrapping of dendrites and lymph space by outer (osc), median (msc), and inner (isc) sheath cells. (c) Close-up of receptor cell soma showing a moderately electron-dense cytoplasm containing the circular nucleus (nu(rc)), slender mitochondria (mi), and loose cisternae of rough endoplasmic reticulum (rER). d. Toluidine-blue stained semi-thin section of proximal third of the tarsus showing several clusters of receptor cells (crc) nested between main sheath cells and interstitial epidermal cells (epc), receptor cell clusters project their axon bundles (axb) proximally, where they converge to form bigger axon bundles (arrow). Note cellular inclusions in tarsal cuticle (cu) containing dendritic (ds + ods) and sheath cell (asc + sc) apparatus. Further labels: de, desmosome (zonula adhaerens); di, distal direction (towards tarsal claw); g, electron-dense granules; mv, microvilli (projected by proximal sheath cell); pro, proximal direction (towards metatarsus); sj, septate junctions [Color figure can be viewed at wileyonlinelibrary.com]

Contact-chemoreceptors in tip-pore sensilla of pterygote insects generally contain fewer numbers of receptor cells, usually between 4 and 6 (e.g., Hansen & Heumann, 1971; Ozaki & Tominaga, 1999; Schmidt & Gnatzy, 1972; Stocker, 1994; Zacharuk, 1980). Located on the antennae, various mouthparts (e.g., labellum of flies), and tarsi of walking legs, these sensilla usually contain four chemoreceptive cells, which cover taste for sugar (one cell), water (one cell), and salt (two cells), according to electrophysiological recordings (e.g., Dethier, 1968; Ozaki & Tominaga, 1999). Electrophysiology and molecular data on contact-chemoreceptors of the vinegar fly *Drosophila melanogaster*

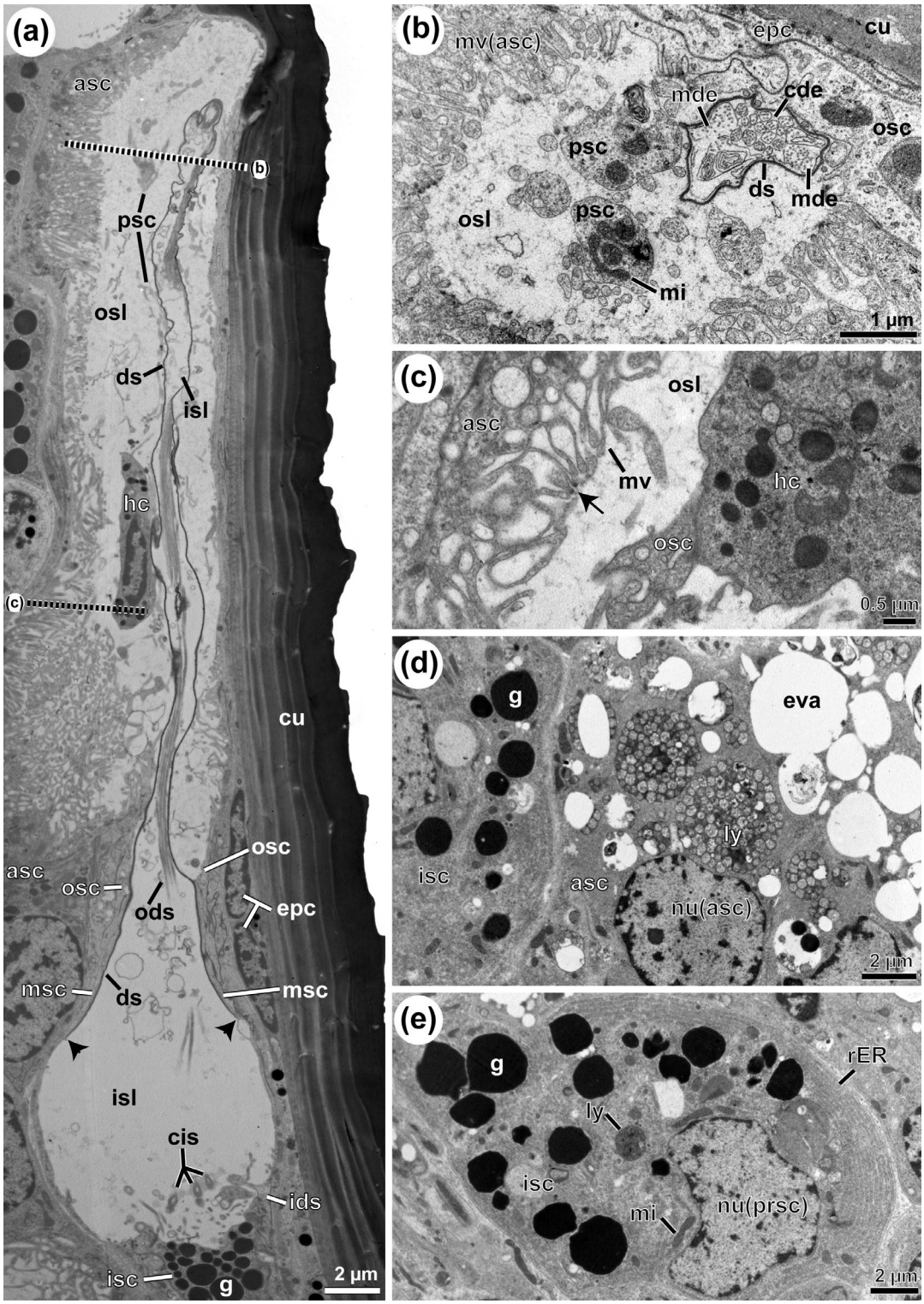

FIGURE 10 Legend on next page.

Meigen, 1830 revealed a remarkable resolution of sweet, bitter/high-salt and low-salt taste modalities as well as a distinct sensitivity for non-volatile pheromones (Ebbs & Amrein, 2007; Ishimoto & Tanimura, 2004; Miyamoto & Amrein, 2014). The much higher number of chemoreceptor cells in trichoid tip-pore sensilla of entelegyne araneomorph spiders may lead to higher taste sensitivity by each cell responding to a wide spectrum of substances. Alternatively, each chemoreceptive cell may respond to a specific spectrum of chemical stimuli. The latter assumption is in line with the electrophysiological recordings on "blunt-tipped hairs" on the walking legs of the spider *Amaurobius similis* (Blackwall, 1861), according to which only 5–6 out of 19 chemoreceptive cells responded positively to taste stimuli like monovalent salts and hydrochloric acid (Harris & Mill, 1977). Harris & Mill (1977) suggested that the chemoreceptors are differentiated in their tasks and might react only to specific substances ("narrow reaction spectrum"). The diversification of chemoreceptors in spiders might also imply detection of volatile pheromones in sensilla that are currently known to function as gustatory sensilla only (based on morphological data).

Indeed, it is known that volatile odours can stimulate chemoreceptors in the tip-pore sensilla of larval and adult insects (Ozaki & Tominaga, 1999) and there is a wealth of electrophysiological recording data on calliphorid/simuliid flies and moths (Dethier, 1972; Städler & Hanson, 1975). Moreover, similar organizational principles regarding the projection targets of receptor neurons in the CNS (e.g., glomerulus-like subcompartments) apply to both olfactory and gustatory sensilla in dipterans such as *Drosophila melanogaster* (Stocker, 1994 and papers cited therein).

The coupling of gustation and olfaction in trichoid tip-pore sensilla has been assumed previously for spiders (e.g., Foelix, 2011; Foelix & Chu-Wang, 1973a) due to the lack of multiporous (wall-pore) sensilla. As we were unable to find wall-pore sensilla, this general conclusion of Foelix and co-workers also applies to *Argiope* spiders. However, combined gustatory and olfactory properties of tip-pore sensilla have not been tested/confirmed yet by electrophysiological recordings. If chemical stimuli, soluble and substrate-bound as well as volatile substances are perceived via the tip-pore sensilla, the substances can only connect to the chemoreceptive terminals via the tip-pore. Perception of volatile substances through a single pore would be highly unusual for terrestrial arthropods. It requires the presence of lipophilic ligand-binding proteins, such as the pheromone-binding protein, general odorant-binding proteins (GOBP1, GOBP2) or chemical sense-related lipophilic ligand-binding protein yet detected in olfactory and gustatory sensilla of silk moths and various dipterans (see Steinbrecht, 1999 and Ozaki & Tominaga, 1999 for review). These ligand-binding proteins contact the olfactory receptors in the membrane of the olfactory dendritic outer segments. In multiporous (wall-pore) sensilla of insects, these receptors are widespread over the dendritic outer segments, thereby increasing the receptive surface. Further increase of receptive surface is achieved by branching of the dendritic outer segments in double-walled multiporous sensilla (Tichy & Barth, 1992). A greater receptive surface is a functional prerequisite to properly smell volatile odours, as they are available at much weaker concentrations in the air than odours dissolved in a liquid (e.g., McIver, Siemicki, & Sutcliffe, 1980). Therefore, how volatile odours can be perceived through a pore at the tip of the sensillum remains a conundrum. It was suggested for bifurcate sensilla of Black flies (*Simulium venustum* Say, 1823) that inner sensillum liquor is discharged and spreads over the surface through a groove adjacent to the tip pore (McIver et al., 1980). Also, an overlay of electron-dense material on the cuticle surrounding the tip-pore of the bowfly *Protophormia terraenovae* Robineau-Desvoidy, 1830 was found, which appears similar to the inner sensillum liquor (Hansen & Heumann, 1971). Such liquors discharged from pores and dispersed over the sensillum shaft's surface may help to adsorb and accumulate these volatile odours. We did not observe inner sensillum lymph material outside the tip pore in *Argiope* spp., but this was occasionally found by Foelix & Chu-Wang (1973a) in *A. diadematus* (Figure 14).

In some spider taxa, such as Mygalomorpha (see Table 1), Theridiidae, and Clubionidae, release of inner sensillum lymph from tip-pore sensilla ("ribbed hair sensilla") located on scopula (adhesive) pads was observed (e.g., Peattie, Dirks, Henriques, & Federle, 2011; Wolff & Gorb, 2016). Once released, receptor lymph may not only coagulate in and around the terminal pore but also extend from the pore forming "trails" (Foelix et al., 2013; Foelix, Rast, & Peattie, 2012;

FIGURE 10 *Argiope bruennichi*, microanatomy of tarsal trichoid tip-pore sensilla (a,c–e: females, b: male), as depicted from longitudinal (a) and cross (b–e) sections. Subcuticular portion of dendritic apparatus and sheath cell system. (a) Panorama overview of almost entire subcuticular portion of outer dendritic segments (ods) and inner sensillum lymph space (isl). At bottom of the inner sensillum lymph space, ciliary region is indicated by ciliary segments (cis). Both sensillum lymph spaces are separated by dendritic sheath (ds), black arrowheads mark the proximal end of the dendritic sheath; voluminous outer sensillum lymph space (osl) is surrounded by numerous accessory sheath cells (asc) and may contain hemocytes (hc). (b) Two large mechanoreceptive dendritic outer segments (mde) flank 16 dendritic outer segments, among them 15 chemoreceptive (cde) and the third, not clearly discernible mechanoreceptive dendrite. Outer sensillum lymph space is lined by microvilli of accessory sheath cells (mv(asc)) and traversed by distal cytoplasmic processes of accessory as well as main (outer and/or median) sheath cells (psc). Section level coincides with a region where the dendritic apparatus becomes bent to take a course strictly subjacent and parallel to the cuticle, indicated in (a) by dashed line. (c) Detail of periphery of outer sensillum lymph space penetrated by microvilli (mv) of accessory sheath cells, microvillar tips are covered by an electron-dense plaque (arrow); note details of granulated hemocyte and outer sheath cell (osc); section plane marked by dashed line in (a). (d) Cytoplasmic organelles of an accessory sheath cell; large, circular vesicles with no obvious contents (eva) are present as well as mosaic-like inclusions resembling early stages of lysosomes (lys). (e) Cytoplasmic composition of the soma of the inner sheath cell (isc) with well-developed rough endoplasmic reticulum (rER), slender mitochondria (mi), and polymorphic granules with extremely electron-dense content (g) (also partly cut in a and d). Further labels: cu, tarsal cuticle; epc, epidermal cells; ids, inner dendritic segment; nu(asc), nucleus of an accessory sheath cell

TABLE 1 Compilation of present knowledge of trichoid tip-pore sensilla on tarsus of pedipalps or walking legs of various spiders. This table combines and enhances previous approaches to homologize constituents of spider tip-pore sensilla, such as the sensory apparatus or system of sheath cell (compare table 2 in Foelix (1985) and table 1 in Hoheisel & Martens (1990)). Original terms of previous authors are put in brackets and/or quotation marks

Reference(s)		Ganske & Uhl (2018) Present paper	Foelix & Chu-Wang (1973a, 1973b) Foelix (1970)	Foelix & Chu-Wang (1973a, 1973b)	Harris & Mill (1973) Harris & Mill (1977) Harris (1977)	Tichy et al. (2001) Barth (2002)	Foelix et al. (2013)
Chelicerate subtaxon		Araneae: Araneomorphae: Araneidae	Araneae: Araneomorphae: Araneidae	Araneae: Araneomorphae: Lycosidae	Araneae: Araneomorphae: Amaraubiidae	Araneae: Araneomorphae: Trechaelidae	Araneae: Mygalomorphae: Teraphosidae
Study species		*Argiope bruennichi* (Scopoli, 1772), *Argiope blanda* O. Pickard-Cambridge, 1898	*Araneus diadematus* (Clerck, 1757)	*Rabidosa punctulata* (Hentz, 1844)	*Amaurobius ferox* (Walckenaer, 1830), *Amaurobius similis* (Blackwall, 1861)	*Cupiennius salei* (Keyserling, 1877)	*Brachypelma albiceps* Pocock, 1903, *Brachypelma smithi* (O. Pickard-Cambridge, 1897), *Tliltocatl albopilosus* (Valerio, 1980)
Sex		Males and females	Males and females	Males and females	Not specified	Males and subadults	Males (and females?)
Study methods		LM, SEM, TEM	LM, SEM, TEM	SEM, TEM	SEM, TEM	SEM, TEM	SEM, TEM
Name of sensillum		Tip-pore sensillum	"Chemosensitive hair", "chemosensitive hair sensillum"	"Chemosensitive hair sensillum"	"Chemoreceptor sensillum", "chemoreceptive hair"	"Tip-pore sensillum", "male spider pheromone sensillum"	"Ribbed hairs", "chemosensory hairs"
Position on the body		Tarsus (first and second walking legs, pedipalps)	Tarsus (walking legs, pedipalps)	Tarsus (walking legs), near-by scopulate hairs	Tarsus, metatarsus ("metatarsal joint")	Tarsus (pedipalps), on dorsal surface	Tarsus (walking legs)
Sensillum shaft	Peridendritic shaft cylinder	Present (penetrated in distal part), partly fused with shaft wall cuticle	Present ("cuticular tube"), partly fused with shaft wall cuticle	Present ("cuticular tube"), centered in sensillum shaft	Present ("inner cuticular tube"), centered in sensillum shaft	Present ("canal", "dendritic sheath"), centered in sensillum shaft	Present ("cuticular tube"), centered in sensillum shaft
	Longitudinal shaft wall canals	Present	Present ("C_3 lumen")	Present ("C_3 lumen")	Present (illustrated on Figure 15)	?	?
	Radial canals in shaft wall cuticle connecting longitudinal canals with outer environment	Not present (?)	Present (illustrated on Figures 13–15 and 16e)	?	?	?	

(Continues)

TABLE 1 (Continued)

Reference(s)		Ganske & Uhl (2018) Present paper	Foelix & Chu-Wang (1973a, 1973b) Foelix (1970)	Foelix & Chu-Wang (1973a, 1973b)	Harris & Mill (1973) Harris & Mill (1977) Harris (1977)	Tichy et al. (2001) Barth (2002)	Foelix et al. (2013)
Receptor cells	Total number receptor cells	5–25	Approximately 22	21–23	Approximately 20	21	12 + x
	Number chemoreceptor cells (including hygroreceptors)	2–22	Approximately 19	Approximately 20	Approximately 18	19	12
	Total number mechanoreceptive cells	2–3	3	1–3	2	2	?
	Number mechanoreceptive dendrites/tubular bodies attached to shaft base	1–2	2	1–3	2	2	?
	Number mechanoreceptive dendrites/tubular bodies attached to peridendritic shaft cylinder	1	1 (illustrated on Figure 11)	?	?	?	?
Main (inner) sheath	Inner sheath cell	Present	? (“enveloping cell 1”?)	? (“enveloping cell 1”)	Present (“inner microvillar cell”)	?	?
	Median sheath cell (= thecogen cell)	Present	Present (“enveloping cell 2”)	? (“enveloping cell 1”)	Present (“sheath cell”)	?	?
	Outer sheath cell (= trichogen cell)	Present	Present (“enveloping cell 3”)	Present (“enveloping cell 2”)	Present (“enveloping cell”)	?	?
Outer (accessory) sheath	Accessory sheath cell(s) (= tormogen cell(s)?)	Present (*n* = 5–12), arranged epithelially	?	Present (“enveloping cell 3”)	Present (*n* = 1—several) (“outer microvillar cell”)	?	?
Inner sensillum lymph space		Present	Present (“C_1 lumen”)	Present (“C_1 lumen”)	Present (“inner extracellular space”)	Present (illustrated on Figure 2c)	Present (illustrated on Figures 1 and 2)
Outer sensillum lymph space		Present	Present (“C_2 lumen”)	Present (“C_2 lumen”)	Present (“outer extracellular space”)	Most likely present (illustrated on Figure 2c)	Most likely present (illustrated on Figures 1 and 2)

Abbreviations: LM, light microscopy; SEM, scanning electron microscopy; TEM, transmission electron microscopy.

Peattie et al., 2011). These "trails" were erroneously considered to be silk threads, serving adhesion (e.g., see Gorb et al., 2006 and rejection by Foelix et al., 2013). Albeit, these findings indicate that small amounts of sensillum lymph are released through the terminal pore of the spider tip-pore sensilla. As with insects, these lymph substances might function as a solvent for chemical substances received by (gustatory) receptors (Wolff & Gorb, 2016).

Re-investigation of the tip-pore region by high pressure freezing for primary fixation as well as serial block-face imaging may help to elucidate whether the odour-catching mechanism is driven by discharged liquors. Possibly, trichoid tip-pore sensilla located further proximally on a spider's leg show these or other characteristics that suggest olfactory functions. Interestingly, differential and location-dependent responses to gustatory and olfactory cues have been recorded from the maxillary tip-pore sensilla (sensilla styloconica) of lepidopteran larvae. Although identical in ultrastructure (Schoonhoven & Dethier, 1966), electrophysiological recordings by Städler & Hanson (1975) revealed that three out of four lateral sensilla styloconica of the moth *Manduca sexta* (Linnaeus, 1763) responded to volatile odours while the medial ones did not.

4.2.2 | Mechanoreceptors

The mechanoreceptive part of the trichoid tip-pore sensilla of *Argiope* spp. contains more receptor cells (n = 2–4, see Table 1) than found in contact-chemoreceptors of various insects (n = 1; e.g., Hansen & Heumann, 1971). This difference suggests that the arachnid tip-pore sensillum is more sensitive to detect bending of the sensillum shaft. However, the specific functional role of the newly described third mechanoreceptive cell in *Argiope* spp. remains unclear. As its tubular body attaches to the proximal end of the peridendritic shaft cylinder rather than to the shaft's base, this additional mechanoreceptor may detect fine scale distortions of the shaft.

5 | CONCLUSIONS

The present paper provides first insights into the microanatomy of tarsal tip-pore sensilla on the first and second walking leg of *A. bruennichi* and *A. blanda* using TEM data. The tip-pore sensilla show variations in the (sub)cellular organization that are not correlated to their location on the tarsus. In many aspects, the sensilla are similar to those described from other spider species but we pinpoint some morphological characters that were not found in previous investigations. That the tip-pore sensilla of *A. bruennichi* are also capable of detecting volatile odours seems likely in light of the similarity found in the sensilla of the tarsus. To adsorb and accumulate volatile odours in a liquid phase around the tip-pore, however, is a pivotal prerequisite of the assumed dual chemoreception. Mechanism of adsorption and accumulation could be similar to those proposed to be effective in tip-pore sensilla of calliphorid and simuliid flies. A combined gustatory and olfactory function would require the presence of a variety of odorant/ligand-binding proteins in the most distal compartment of the inner sensillum lymph space below the tip-pore. A comprehensive future study is needed targeting potential anatomical differences between tip-pore sensilla of the tarsus and podomers situated further proximally on the spider legs and pedipalps (TEM), testing chemical stimuli using single cell recording (electrophysiology), elucidating the identity and location of odorant/ligand-binding proteins (immunocytochemistry, proteomics), and the diversity of receptor proteins (receptor genetics).

ACKNOWLEDGEMENTS

The authors are grateful to Matthes Kenning who contributed SEM images and conducted a morphometric analysis of shaft surface structures. For fruitful discussions and references, the authors are indebted to Jonas Wolff and Peter Michalik (Greifswald). Open access funding enabled and organized by Projekt DEAL.

CONFLICT OF INTEREST

The authors declare no conflict of interest.

AUTHOR CONTRIBUTIONS

Carsten H. G. Müller and **Gabriele Uhl**: Planned and designed the study. **Carsten H. G. Müller**: Carried out the TEM including the analysis, interpretation of the TEM data and produced all figure plates. **Anne-Sarah Ganske**: Contributed various SEM images. **Carsten H. G. Müller** and **Gabriele Uhl**: Wrote the manuscript. All authors read and approved the final version of the manuscript.

PEER REVIEW

The peer review history for this article is available at https://publons.com/publon/10.1002/jmor.21276.

DATA AVAILABILITY STATEMENT

Raw data are available from the corresponding author upon request.

ORCID

Carsten H. G. Müller https://orcid.org/0000-0001-6644-6177
Gabriele Uhl https://orcid.org/0000-0001-8758-7913

REFERENCES

Altner, A., & Loftus, R. (1985). Ultrastructure and function of insect thermo- and hygroreceptors. *Annual Reviews of Entomology*, *30*, 273–295.

Altner, H., & Prillinger, L. (1980). Ultrastructure of invertebrate chemo-, thermo-, and hygroreceptors and its functional significance. *International Review of Cytology*, *67*, 69–139.

Anton, S., & Tichy, H. (1994). Hygro- and thermoreceptors in tip-pore sensilla of the tarsal organ of the spider *Cupiennius salei*: Inervation and central projection. *Cell Tissue Research*, *278*, 399–407.

Barth, F. G. (2002). *A spider's world—Senses and behavior*. Berlin, Germany: Springer.

Blanke, R. (1973). Nachweis von Pheromonen bei Netzspinnen. *Journal of Zoology*, *246*, 21–27.

Chinta, S. P., Goller, S., Lux, J., Funke, S., Uhl, G., & Schulz, S. (2010). The sex pheromone of the wasp spider *Argiope bruennichi*. *Angewandte Chemie*, *49*, 2033–2036.

Dethier, V. G. (1968). Chemosensory input and taste discrimination in the blowfly. *Science*, *161*, 389–391.

Dethier, V. G. (1972). Sensitivity of the contact chemoreceptors of the blowfly to vapors. *Proceedings of the National Academy of Sciences of the United States of America*, *69*, 2189–2192.

Dumpert, K. (1978). Spider odor receptor: Electrophysiological proof. *Experientia*, *34*, 754–755.

Ebbs, M. L., & Amrein, H. (2007). Taste and pheromone perception in the fruit fly *Drosophila melanogaster*. *European Journal of Physiology*, *454*, 735–747.

Ehn, R., & Tichy, H. (1994). Hygro- and thermoreceptive tarsal organ in the spider *Cupiennius salei*. *Journal of Comparative Physiology A*, *174*, 345–350.

Erickson, R. P. (1963). Sensory neural patterns and gustation. In Y. Zotterman (Ed.), *Olfaction and taste* (Vol. 1, pp. 205–213). New York, NY: Pergamon Press.

Farley, R. D. (1999). Scorpiones. In F. W. Harrison & R. F. Foelix (Eds.), *Microscopic anatomy of invertebrates, chelicerate Arthropoda* (Vol. 8A, pp. 117–222). New York, NY: Wiley-Liss.

Fischer, A., Lee, Y., Stewart, J., & Gries, G. (2019). Dodging sexual conflict? Sub-adult females of a web-building spider stay cryptic to mate-seeking adult males. *Ethology*, *124*, 838–843.

Foelix, R., Erb, B., & Rast, B. (2013). Alleged silk spigots on tarantula feet: Electron microscopy reveals sensory innervation, no silk. *Arthropod Structure & Development*, *42*, 209–217.

Foelix, R., Rast, B., & Peattie, A. M. (2012). Silk secretion from tarantula feet revisited: Alleged spigots are probably chemoreceptors. *The Journal of Experimental Biology*, *215*, 1084–1089.

Foelix, R. F. (1970). Chemosensitive hairs in spiders. *Journal of Morphology*, *132*, 313–334.

Foelix, R. F. (1985). Mechano- und chemoreceptive sensilla. In F. G. Barth (Ed.), *Neurobiology of spiders* (pp. 118–137). Berlin, Germany: Springer.

Foelix, R. F. (2011). *The biology of spiders* (3rd ed.). Oxford, England: Oxford University Press.

Foelix, R. F. (2015). *Biologie der Spinnen* (3rd ed.). Chimaira: Frankfurt a.M.

Foelix, R. F., & Axtell, R. C. (1972). Ultrastructure of Haller's organ in the tick *Amblyomma americanum* L. *Cell Tissue Research*, *124*, 275–292.

Foelix, R. F., & Chu-Wang, I.-W. (1973a). The morphology of spider sensilla. II. Chemoreceptors. *Tissue & Cell*, *5*, 461–478.

Foelix, R. F., & Chu-Wang, I.-W. (1973b). The morphology of spider sensilla. I. Mechanoreceptors. *Tissue & Cell*, *5*, 451–460.

Foelix, R. F., Chu-Wang, I. W., & Beck, L. (1975). Fine structure of tarsal sensory organs in the whip spider *Admetus pumilio* (Amblypygi, Arachnida). *Tissue and Cell*, *7*, 331–346.

Forster, R. R. (1980). Evolution of the tarsal organ, the respiratory system and the female genitalia in spiders. In: J. Gruber (Ed). Proceedings of the 8th International Congress on Arachnology, pp. 269–284. Verlag H. Engermann: Vienna, Austria.

Forster, R. R., Platnick, N. I., & Gray, M. R. (1987). A review of the spider superfamilies Hypochiloidea and Austrochiloidea (Araneae, Araneomorphae). *Bulletin of the American Museum of Natural History*, *185*, 1–116.

Gainett, G., Michalik, P., Müller, C. H. G., Giribet, G., Talarico, G., & Willemart, R. H. (2017). Ultrastructure of chemoreceptive tarsal sensilla in an armored harvestman and evidence of olfaction across Laniatores (Arachnida, Opiliones). *Arthropod Structure & Development*, *46*, 178–195.

Ganske, A.-S., & Uhl, G. (2018). The sensory equipment of a spider—A morphological survey of different types of sensillum in both sexes of *Argiope bruennichi* (Araneae, Araneidae). *Arthropod Structure & Development*, *47*, 144–161.

Gaskett, A. (2007). Spider sex pheromones: Emission, reception, structures, and functions. *Biological Reviews*, *82*, 27–48.

Gorb, S. N., Niederegger, S., Hayashi, C. Y., Summers, A. P., Vötsch, W., & Walther, P. (2006). Biomaterials: Silk-like secretion from tarantula feet. *Nature*, *443*, 407.

Hallberg, E., & Skog, M. (2011). Chemosensory sensilla in crustaceans. In T. Breithaupt & M. Thiel (Eds.), *Chemical communication in crustaceans* (pp. 103–121). Berlin, Germany: Springer.

Hansen, K., & Heumann, H.-G. (1971). The fine structure of the tarsal taste hairs of the blowfly *Phormia terraenovae* Rob.-Desv. *Cell Tissue Research*, *117*, 419–442.

Harris, D. J. (1977). Hair regeneration during moulting in the spider *Ciniflo similis* (Araneae, Dictynidae). *Zoomorphology*, *88*, 37–63.

Harris, D. J., & Mill, P. J. (1973). The ultrastructure of chemoreceptor sensilla of *Ciniflo* (Araneida: Arachnida). *Tissue & Cell*, *5*, 679–689.

Harris, D. J., & Mill, P. J. (1977). Observations on the leg receptors of *Ciniflo* (Araneida: Dictynidae). II. Chemoreceptors. *Journal of Comparative Physiology*, *119*, 55–62.

Hess, E., & Vlimant, M. (1982). The tarsal sensory system of *Amblyomma variegatum* Fabricius (Ixodidae, Metastriata). I. Wall pore and terminal pore sensilla. *Revue Suisse de Zoologie*, *89*, 713–729.

Hoheisel, U., & Martens, J. (1990). The compound sensilla on the ovipositor of Phalangium opilio Linné (Arachnida: Opiliones: Phalangiidae). Zoologische Jahrbücher (Abteilung Anatomie), 120, 63–79.

Hunger, T., & Steinbrecht, R. A. (1998). Functional morphology of a double-walled multiporous olfactory sensillum: The sensillum coeloconicum of *Bombyx mori* (Insecta, Lepidoptera). *Tissue & Cell*, *30*, 14–29.

Ishimoto, H., & Tanimura, T. (2004). Molecular neurophysiology of taste in *Drosophila*. *Cellular and Molecular Life Sciences*, *61*, 10–18.

Iwasaki, M., Itoh, T., & Tominaga, Y. (1999). Mechano- and phonoreceptors. In E. Eguchi & Y. Tominaga (Eds.), *Atlas of arthropod sensory receptors. Dynamic morphology in relation to function* (pp. 177–190). Tokyo, Japan: Springer.

Karnovsky, M. J. (1965). A formaldehyde-glutaraldehyde fixative of high osmolality for use in electron microscopy. *Journal of Cell Biology*, *27*, 137–138.

Keil, T. A. (2012). Sensory cilia in arthropods. *Arthropod Structure & Development*, *41*, 515–534.

Keil, T. A., & Steinbrecht, R. A. (1984). Mechanosensitive and olfactory sensilla of insects. In R. C. King & H. Akai (Eds.), *Insect Ultrastructure* (Vol. 2, pp. 477–516). Plenum Press: New York, NY.

Kronestedt, T. (1979). Study on chemosensitive hairs in wolf spiders (Araneae, Lycosidae) by scanning electron microscopy. *Zoologica Scripta*, *8*, 279–285.

McIver, S., Siemicki, R., & Sutcliffe, J. (1980). Bifurcate sensilla on the tarsi of female black flies, *Simulium venustum* (Diptera: Simuliidae): Contact chemoreception adapted for olfaction? *Journal of Morphology*, *165*, 1–11.

Meinecke, C.-C. (1975). Olfactory sensilla and systematic of the Lamellicornia (Insecta, Coleoptera). *Zoomorphology*, *82*, 1–42.

Miyamoto, T., & Amrein, H. (2014). Diverse roles for the *Drosophila* fructose sensor Gr43a. *Fly*, *8*, 19–25.

Morita, H. (1992). Transduction process and impulse initiation in insect contact chemoreceptor. *Zoological Science*, *9*, 1–16.

Müller, C. H. G., & Sombke, A. (2015). Diplopoda—Sense organs. In A. Minelli (Ed.), *The Myriapoda Treatise on zoology—Anatomy, taxonomy, biology* (Vol. 2, pp. 181–235). Brill: Leiden, the Netherlands.

Müller, C. H. G., Sombke, A., Hilken, G., & Rosenberg, J. (2011). Chilopoda—Sense organs (chapter 12). In A. Minelli (Ed.), *The Myriapoda Treatise on zoology—Anatomy, taxonomy, biology* (Vol. 1, pp. 235–278). Brill: Leiden, the Netherlands.

Ninomiya, M., Ozaki, M., Kashihara, Y., & Morita, H. (1986). Destruction and reorganization of the receptor membrane in labellar chemosensory cells of the blowfly: Recovery of response to sugars after destruction. *The Journal of General Physiology*, *87*, 1003–1016.

Ozaki, M., Ninomiya, M., Kashihara, Y., & Morita, H. (1986). Destruction and reorganization of the receptor membrane in labellar chemosensory cells of the blowfly: Long-lasting latent action of colchicine. *The Journal of General Physiology*, *87*, 533–549.

Ozaki, M., & Tominaga, Y. (1999). Contact chemoreceptors. In E. Eguchi & Y. Tominaga (Eds.), *Atlas of arthropod sensory receptors. Dynamic morphology in relation to function* (pp. 143–154). Tokyo, Japan: Springer.

Peattie, A. M., Dirks, J.-H., Henriques, S., & Federle, W. (2011). Arachnids secrete a fluid over their adhesive pads. *PLoS One*, *6*(5), e20485.

Pfreundt, C., & Peters, W. (1981). Die Verteilung von chemosensorischen Haaren auf Laufbeinen von Spinnen mit unterschiedlicher Lebensweise. *Zoologische Beiträge (N.F.)*, *27*, 335–349.

Rees, C. J. C. (1967). Transmission of receptor potential in dipteran chemoreceptors. *Nature*, *215*, 301–302.

Richardson, K. C., Jarett, L., & Finke, E. H. (1960). Embedding in epoxy resins for ultrathin sectioning in electron microscopy. *Stain Technology*, *35*, 313–323.

Ross, K., & Smith, R. (1979). Aspects of the courtship behavior of the black widow spider, *Latrodectus hesperus* (Araneae: Theridiidae), with evidence for the existence of a contact sex pheromone. *Journal of Arachnology*, *7*, 69–77.

Schmidt, K., & Gnatzy, W. (1972). The fine structure of the sensory hairs on the cerci of *Gryllus bimaculatus* Deg. (Saltatoria, Gryllidae). III. The short bristles. I. *Cell and Tissue Research*, *126*, 206–222.

Schneider, J., Uhl, G., & Herberstein, M. E. (2015). Cryptic female choice within the genus *Argiope*: A comparative approach. In A. V. Peretti & A. Aisenberg (Eds.), *Cryptic female choice in arthropods. Patterns, mechanisms and prospects* (pp. 55–77). Heidelberg, Germany: Springer.

Schoonhoven, L. M., & Dethier, V. G. (1966). Sensory aspects of host-plant discrimination by lepidopterous larvae. *Archives Néérlandaises de de Zoologie*, *16*, 497–530.

Städler, E., & Hanson, F. E. (1975). Olfactory capabilities of gustatory chemoreceptors of tobacco hornworm larvae. *Journal of Comparative Physiology A*, *104*, 97–102.

Steinbrecht, R. A. (1984). Chemo-, hygro-, and thermoreceptors. In J. Bereiter-Hahn, A. G. Matoltsy, & K. S. Richards (Eds.), *Biology of the integument 1—Invertebrates* (pp. 523–553). Berlin, Germany: Springer.

Steinbrecht, R. A. (1997). Pore structures in insect olfactory sensilla: A review of data and concepts. *International Journal of Insect Morphology and Embryology*, *26*, 229–245.

Steinbrecht, R. A. (1999). Olfactory receptors. In E. Eguchi & Y. Tominaga (Eds.), *Atlas of arthropod sensory receptors. Dynamic morphology in relation to function* (pp. 155–176). Tokyo, Japan: Springer.

Stengl, M. (2019). Chemosensory transduction in arthropods. In J. H. Byrne (Ed.), *The Oxford handbook of invertebrate neurobiology. Subject neuroscience, invertebrate neurobiology, molecular and cellular systems* (pp. 1–38). Oxford: Oxford University Press.

Stocker, R. F. (1994). The organization of the chemosensory system in *Drosophila melanogaster*: A review. *Cell Tissue Research*, *275*, 3–36.

Symonds, M. R., & Elgar, M. A. (2008). The evolution of pheromone diversity. *Trends in Ecology & Evolution*, *23*, 22–228.

Talarico, G., Palacios-Vargas, J. G., & Alberti, G. (2008). The pedipalp of *Pseudocellus pearsei* (Ricinulei, Arachnida) – Ultrastructure of a multifunctional organ. *Arthropod Structure & Development*, *37*, 511–521.

Talarico, G., Palacios-Vargas, J. G., Fuentes Silva, M., & Alberti, G. (2006). Ultrastructure of tarsal sensilla and other integument structures of two *Pseudocellus* species (Ricinulei, Arachnida). *Journal of Morphology*, *267*, 441–463.

Thurm, U., Erler, G., Gödde, J., Kastrup, H., Keil, T., Völker, W., & Vohwinkel, B. (1983). Cilia specialized for mechanoreception. *Journal of Submicroscopic Cytology*, *15*, 151–155.

Tichy, H., & Barth, F. G. (1992). Fine structure of olfactory sensilla in myriapods and arachnids. *Microscopy Research and Techniques*, *22*, 372–391.

Tichy, H., Gingl, E., Ehn, R., Papke, M., & Schulz, S. (2001). Female sex pheromone of a wandering spider (*Cupiennius salei*): Identification and sensory reception. *Journal of Comparative Physiology A*, *187*, 75–78.

Tichy, H., & Loftus, R. (1996). Hygroreceptors in insects and a spider: Humidity transduction models. *The Science of Nature*, *83*, 255–263.

Uhl, G. (2013). Spider olfaction: Attracting, detecting, luring and avoiding. In W. Nentwig (Ed.), *Spider ecophysiology* (pp. 141–157). Berlin, Germany: Springer.

Uhl, G., & Elias, D. O. (2011). Communication. In M. E. Herberstein (Ed.), *Spider behaviour, flexibility and versatility* (pp. 127–188). Cambridge, England: Cambridge University Press.

Witt, P. N. (1982). Communication in spiders. In P. N. Witt & J. Rovner (Eds.), *Spider communication: Mechanisms and ecological significance* (pp. 3–14). Princeton, NJ: Princeton University Press.

Wolff, J. O., & Gorb, S. N. (2016). Adhesive secretions (chapter 8). In J. O. Wolff & S. N. Gorb (Eds.), *Attachment structures and adhesive secretions in arachnids Biologically-inspired systems* (Vol. 7, pp. 117–140). Heidelberg, Germany: Springer.

Wyatt, T. D. (2003). *Pheromones and animal behaviour: Communication by smell and taste*. Cambridge, England: Cambridge University Press.

Yokohari, F. (1999). Hygro- and thermoreceptors. In E. Eguchi & Y. Tominaga (Eds.), *Atlas of arthropod sensory receptors. Dynamic morphology in relation to function* (pp. 191–210). Tokyo, Japan: Springer.

Zacharuk, R. Y. (1980). Ultrastructure and function of insect chemosensilla. *Annual Reviews of Entomology*, *25*, 27–47.

SUPPORTING INFORMATION

Additional supporting information may be found online in the Supporting Information section at the end of this article.

How to cite this article: Müller CHG, Ganske A-S, Uhl G. Ultrastructure of chemosensory tarsal tip-pore sensilla of *Argiope* spp. Audouin, 1826 (Chelicerata: Araneae: Araneidae). *Journal of Morphology*. 2020;281:1634–1659. https://doi.org/10.1002/jmor.21276